



## Supplementary Materials for

### **Evidence for a Common Mechanism of SIRT1 Regulation by Allosteric Activators**

Basil P. Hubbard, Ana P. Gomes, Han Dai, Jun Li, April W. Case, Thomas Considine,  
Thomas V. Riera, Jessica E. Lee, Sook Yen E, Dudley W. Lamming, Bradley L. Pentelute,  
Eli R. Schuman, Linda A. Stevens, Alvin J. Y. Ling, Sean M. Armour, Shaday Michan,  
Huizhen Zhao, Yong Jiang, Sharon M. Sweitzer, Charles A. Blum, Jeremy S. Disch, Pui Yee Ng,  
Konrad T. Howitz, Anabela P. Rolo, Yoshitomo Hamuro, Joel Moss, Robert B. Perni,  
James L. Ellis, George P. Vlasuk, David A. Sinclair\*

\*To whom correspondence should be addressed. E-mail: david\_sinclair@hms.harvard.edu

Published 8 March 2013, *Science* **339**, 1216 (2013)  
DOI: 10.1126/science.1231097

#### **This PDF file includes:**

Materials and Methods

Figs. S1 to S20

Tables S1 to S8

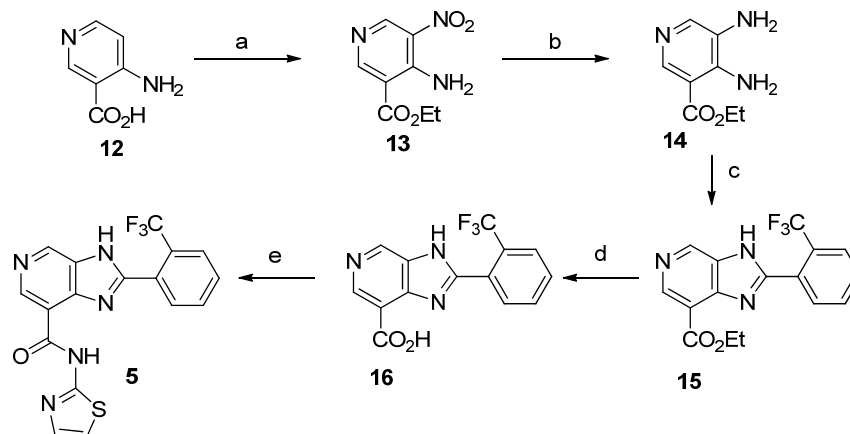
References

## **Materials and Methods**

### Preparation of STAC-5 to 10

*General Experimental:* Reagents were obtained from commercial sources and were used as received. All reactions were run under an inert atmosphere (N<sub>2</sub>). Unless otherwise indicated, chromatography refers to medium pressure chromatography performed on an ISCO Combiflash Rf System. <sup>1</sup>H NMR spectra were obtained on either a Varian Mercury Plus 300 MHz or a Bruker Advance III 300 MHz spectrometer and referenced to internal TMS (0.00 ppm), CHCl<sub>3</sub> (7.26 ppm), or DMSO (2.49 ppm). NMR spectral data are reported as follows: chemical shift (δ) in ppm, (multiplicity, coupling constants in Hertz, number of protons). Multiplicity abbreviations are as follows: s-singlet, d-doublet, t-triplet, q-quartet, m-multiplet, br-broad. Low Resolution Mass Spectral data were recorded using an Agilent 1100 series spectrometer integrated into an Agilent 1200 series HPLC system. ESI refers to electrospray ionization. High-resolution mass spectra were determined on a Waters QTOF Premiere system.

*Scheme 1: Preparation of STAC-5*



*a) KNO<sub>3</sub>, H<sub>2</sub>SO<sub>4</sub>; b) H<sub>2</sub>, 10% Pd/C, MeOH; c) 2-trifluoromethylbenzaldehyde, Na<sub>2</sub>S<sub>2</sub>O<sub>5</sub>, DMF; 120°C; d) NaOH, EtOAc, reflux; e) thiazol-2-amine, HATU, DIPEA, DMF.*

**4-Amino-5-nitro-nicotinic acid ethyl ester (13)**

To a stirred solution of **12** (27.6 g, 200 mmol) in concentrated H<sub>2</sub>SO<sub>4</sub> (200 mL) at 0°C was added potassium nitrate (20.5 g, 200 mmol). The resulting mixture was stirred at 0°C for 30 min and then 75°C for 3 hrs. The reaction was allowed to cool to ambient temperature and EtOH was added (540 mL). The resulting mixture was stirred at 60°C for 18 hrs and then slowly added to an ice-cold solution of potassium acetate (800 g, in 1.5 L of water). The resulting precipitate was collected by filtration, washed with water and dried over Na<sub>2</sub>SO<sub>4</sub> to afford **13** (14.6 g, 35%). This material was used without further

purification.  $^1\text{H NMR}$  ( $\text{CDCl}_3$ ):  $\delta$  9.31(s, 1H), 9.07 (s, 1H), 9.05 (br, 1H), 8.28 (br, 1H), 4.42 (q, 2H), 1.43 (t, 3H). MS (ESI) calcd for  $\text{C}_8\text{H}_{10}\text{N}_3\text{O}_4$  (m/z): 212.07, found: 211.92.

#### **4,5-Diamino-nicotinic acid ethyl ester (14)**

A mixture of **13** (15 g, 71 mmol) and 10% Pd/C (500 mg) in MeOH (500 mL) was stirred under 1 atm of hydrogen at ambient temperature for 18 hrs. The resulting mixture was filtered through celite and concentrated to afford **14** (10 g, 80%) which was used in the following step without additional purification.  $^1\text{H NMR}$  ( $\text{CDCl}_3$ ):  $\delta$  8.62 (s, 1H), 7.96 (s, 1H), 6.14 (br, 2H), 4.36 (q, 2H), 3.15 (br, 2H), 1.40 (t, 3H).

#### **2-(2-Trifluoromethyl-phenyl)-3H-imidazo[4,5-c]pyridine-7-carboxylic acid ethyl ester (15)**

A mixture of **14** (1.81 g, 10 mmol), trifluoromethylbenzaldehyde (1.9 g, 11 mmol) and  $\text{Na}_2\text{S}_2\text{O}_5$  (9.5 g, 50 mmol) in DMF (50 mL) was stirred at  $120^\circ\text{C}$  for 18 hrs. The resulting mixture was allowed to cool to ambient temperature and poured into cold water (100 mL). The resulting solid was filtered, washed with water and dried *in vacuo* to provide **15** (2.35 g, 70%), which was used in the subsequent step without additional purification.

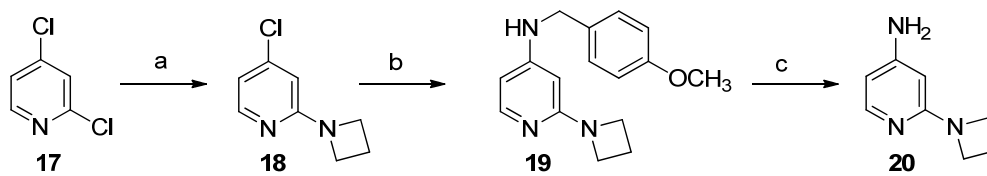
#### **2-(2-Trifluoromethyl-phenyl)-3H-imidazo[4,5-c]pyridine-7-carboxylic acid (16)**

A solution of **15** (2.35 g, 7 mmol) in 10% aqueous NaOH (40 mL) and ethanol (20 mL) was heated at reflux for 30 min. The resulting mixture was allowed to cool to ambient temperature and acidified with 5N aqueous HCl. The resulting yellow solid was filtered, washed with water and dried in vacuo to afford **16** (1.77 g, 85%). <sup>1</sup>H NMR (d<sub>6</sub>-DMSO): δ 13.4 (br, 1H), 9.18 (s, 1H), 8.87 (s, 1H), 7.95 (m, 1H), 7.82 (m, 3H). MS (ESI) calcd for C<sub>14</sub>H<sub>9</sub>F<sub>3</sub>N<sub>3</sub>O<sub>2</sub> (m/z): 308.06, found: 308.0.

**N-(Thiazol-2-yl)-2-(2-trifluoromethyl-phenyl)-3H-imidazo[4,5-c]pyridine-7-carboxamide (**5**)**

A mixture of **16** (64.0 mg, 0.21 mmol), HATU (160 mg, 0.42 mmol), DIPEA (70 μL, 0.42 mmol) and thiazol-2-amine (21.0 mg, 0.21 mmol) in DMF (2 mL) was stirred at room temperature for 18 hrs. The solvent was removed in vacuo and the residue was purified by chromatography (dichloromethane/MeOH 50:1 to 5:1 gradient) to give **5** (10 mg, 12 %) as a pale yellow solid. <sup>1</sup>HNMR (CH<sub>3</sub>OD): δ 9.1(s, 2H), 8.00 (d, 1H), 7.94 (d, 1H), 7.90-7.85 (m, 2H), 7.49 (d, 1H), 7.22 (d, 1H). HRMS calcd for C<sub>17</sub>H<sub>11</sub>N<sub>5</sub>OSF<sub>3</sub> (m/z): 390.0634, found: 390.0635.

*Scheme 2*



*a) Azetidine hydrochloride, K<sub>2</sub>CO<sub>3</sub>, DMSO; b) 4-methoxybenzylamine, Pd<sub>2</sub>(dba)<sub>3</sub>, BINAP, NaOtBu, CH<sub>2</sub>Cl<sub>2</sub>; c) TFA, CH<sub>2</sub>Cl<sub>2</sub>.*

### **2-(Azetidin-1-yl)-4-chloropyridine (18)**

A mixture of **17** (10.0 g, 68 mmol), azetidine hydrochloride (6.3 g, 68 mmol) and K<sub>2</sub>CO<sub>3</sub> (23.3 g, 169 mmol) in DMSO (100 mL) was stirred at 100°C for 12 hrs. Water (150 mL) was added and the mixture was extracted with EtOAc (3 x 100 mL). The combined extracts were washed with brine (3 x 100 mL) and dried over Na<sub>2</sub>SO<sub>4</sub>. Concentration afforded **18** (10.5 g), which was used without further purification in the next step.

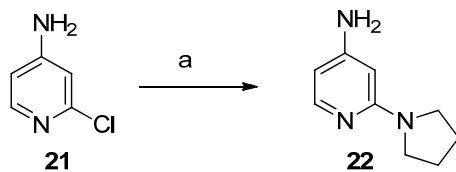
### **2-(Azetidin-1-yl)-N-(4-methoxybenzyl)pyridin-4-amine (19)**

A mixture of **18** (1.68 g, 10.0 mmol), 4-methoxybenzylamine (1.35 g, 10.0 mmol), Pd<sub>2</sub>(dba)<sub>3</sub> (0.27 g, 0.29 mmol), BINAP (0.37 g, 0.60 mmol) and sodium t-butoxide (1.12 g, 10.0 mmol) in dichloromethane (20 mL) was stirred at 110°C for 12 hrs. Water (100 mL) was added and after the layers were separated the organic portion was washed with water (3 x 50 mL), dried over Na<sub>2</sub>SO<sub>4</sub> and concentrated. The residue was purified by chromatography (pet ether/EtOAc 5:1) to afford **19** (2.60 g, 9.7 mmol) as a yellow oil, which was used in the subsequent step without additional purification.

## 2-(Azetidin-1-yl)pyridin-4-amine (**20**)

A solution of **19** (2.5 g, 9.3 mmol) and TFA (20 mL) in dichloromethane (40 mL) was stirred at ambient temperature for 3h. The pH was adjusted to 9 by addition of Na<sub>2</sub>CO<sub>3</sub> and the resulting mixture was extracted with EtOAc (3 x 50 mL). The combined extracts were dried over Na<sub>2</sub>SO<sub>4</sub>, concentrated and chromatographed (pet ether/EtOAc 1:1) to give **20** (50 mg, 4%) as a white solid. <sup>1</sup>H NMR (CDCl<sub>3</sub>): δ 7.84 (d, 1H), 5.96 (d, 1H), 5.49 (s, 1H), 3.98 (m, 6H), 2.34 (q, 2H); MS (ESI) calcd for C<sub>8</sub>H<sub>12</sub>N<sub>3</sub> (m/z): 150.10, found: 150.1.

### Scheme 3



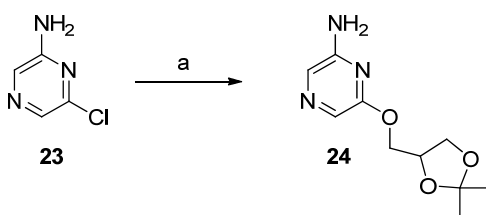
a) Pyrrolidine, K<sub>2</sub>CO<sub>3</sub>, 190°C.

## 2-(Pyrrolidin-1-yl)pyridin-4-amine (**22**)

A mixture of **21** (19.3 g, 150 mmol), K<sub>2</sub>CO<sub>3</sub> (41.7 g, 300 mmol), and pyrrolidine (38.9 g mL, 450 mmol) was stirred at 190°C for 10 hrs. The reaction mixture was allowed to cool to ambient temperature and water (300 mL) was added. The resulting mixture was extracted with EtOAc (4 x 150 mL). The combined extracts were washed with water (3 x 25 mL), dried over Na<sub>2</sub>SO<sub>4</sub> and concentrated. The residue was purified by chromatography (pet ether/ EtOAc 10:1) to afford **22** as a white solid. <sup>1</sup>H NMR (CDCl<sub>3</sub>):

$\delta$  7.86 (d, 1H), 5.92 (m, 1H), 5.89 (d, 1H), 3.92 (br, 2H), 3.41 (m, 4H), 1.97 (m, 4H); MS (ESI) calcd for C<sub>9</sub>H<sub>14</sub>N<sub>3</sub> (m/z): 164.12, found: 164.1.

*Scheme 4*



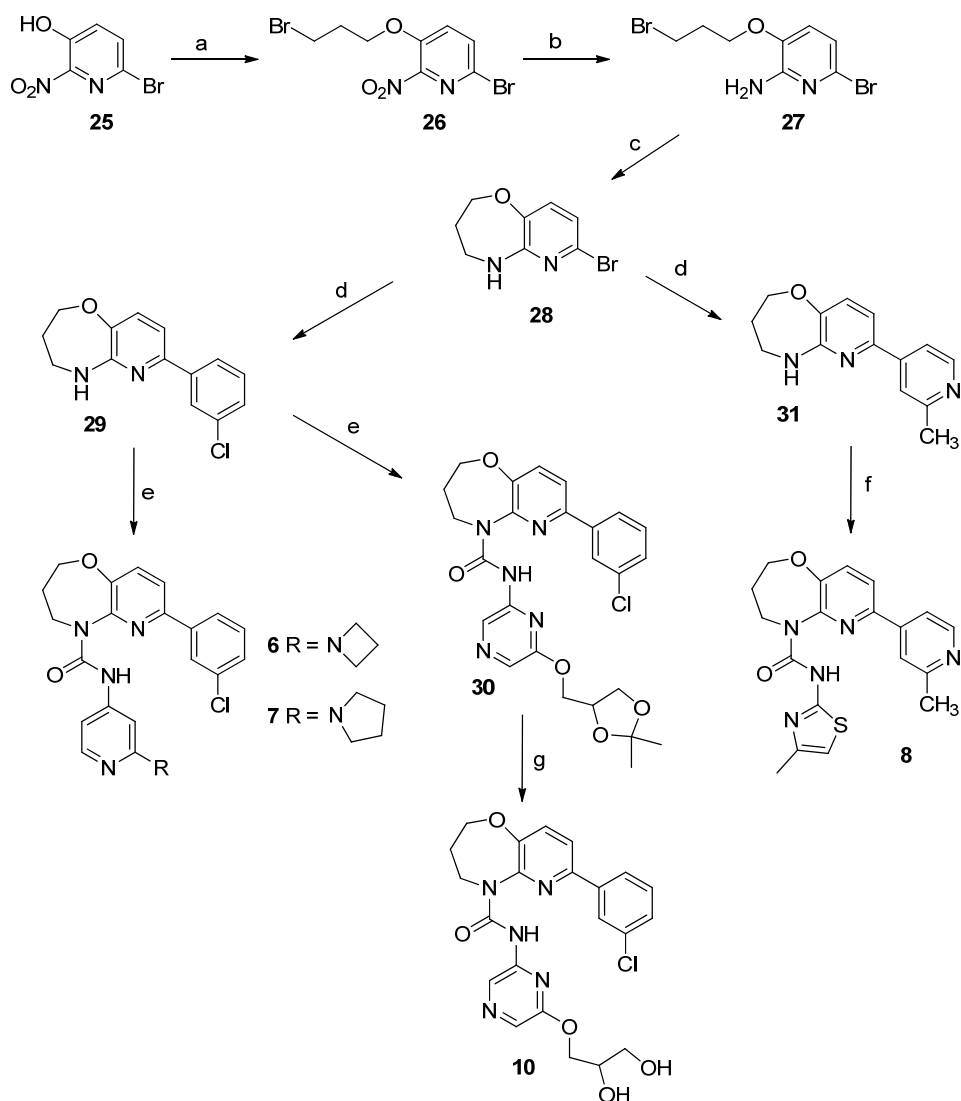
*a)* (2,2-dimethyl-1,3-dioxolane-4-yl)  
methanol, NaH (mineral oil  
suspension), 1,4-dioxane.

#### **6-((2,2-Dimethyl-1,3-dioxolan-4-yl)methoxy)pyrimidin-2-amine (24)**

To a solution of (2,2-dimethyl-1,3-dioxolane-4-yl)methanol (19.5 g, 150 mmol) in 1,4-dioxane (250 mL) at ambient temperature was added NaH (6.0 g, 60% oil suspension) and the resulting mixture was stirred for 30 min. To the reaction was added **23** (6.43 g, 50 mmol) and the resulting mixture was heated to reflux for 48 hrs. The reaction mixture was allowed to cool to ambient temperature and water was added. The mixture was extracted with EtOAc (3 x 100 mL). The combined extracts were washed with water (6 x 50 mL), dried over Na<sub>2</sub>SO<sub>4</sub> and concentrated. The crude product was chromatographed (dichloromethane/MeOH 20:1) to afford **24** (5.7 g, 51%). <sup>1</sup>H NMR (CDCl<sub>3</sub>):  $\delta$  7.61 (s, 1H), 7.54 (s, 1H), 4.47 (q, 1H), 4.41 (br, 2H), 4.23-4.33 (m, 2H), 4.12-4.17 (m, 1H),

3.84-3.88 (m, 1H), 1.46 (s, 3H), 1.40 (s, 3H); MS (ESI) calcd for C<sub>10</sub>H<sub>16</sub>N<sub>3</sub>O<sub>3</sub> (m/z):  
226.12, found: 226.1.

*Scheme 5: Preparation of STAC-6, STAC-7, STAC-8, and STAC-10*



a) 6-Bromo-2-nitropyridine-3-ol, DIAD, PPh<sub>3</sub>, THF; b) Fe (powder), AcOH; c) NaH (mineral oil suspension), THF, 0°C; d) (3-(trifluoromethyl)phenyl) boronic acid or (2-methylpyridin-4-yl)boronic acid, PdCl<sub>2</sub>(dppf), Cs<sub>2</sub>CO<sub>3</sub>, 1,4-dioxane, 80°C; e) **20**, **22**, or **24**, triphosgene, TEA, THF, 60°C; f) phenyl (4-methylthiazol-2-yl)carbamate, DIEA, DMSO, 60°C; g) 12N HCl, THF.

### **6-Bromo-3-(3-bromo(bromopropoxy)-2-nitropyridine (26)**

To a solution of triphenylphosphine (3.93 g, 15 mmol) in THF (22 mL) at 0°C was added dropwise DIAD (3.0 g, 15 mmol). The reaction was stirred for 30 min and added to a solution of 6-bromo-2-nitropyridine-3-ol (**25**) (2.19 g, 10 mmol) and 3-bromopropane-1-ol (2.1g, 15 mmol) in THF (18 mL). The reaction was allowed to warm to ambient temperature and stirred for 2 hrs. The reaction mixture was concentrated and the residue partitioned between EtOAc and water. The organic portion was washed with water, then brine, dried over Na<sub>2</sub>SO<sub>4</sub>, filtered and concentrated. The crude product was purified by silica gel chromatography (EtOAc/pet ether) to give **26** (1.18 g, 35%). <sup>1</sup>H NMR (CDCl<sub>3</sub>): δ 7.70 (d, J=8.7Hz, 1H), 7.46 (d, J=8.4Hz, 1H), 4.30 (t, 2H), 3.61 (t, 2H), 2.39 (m, 2H).

### **6-Bromo-3-(3-bromopropoxy)pyridine-2-amine (27)**

A mixture of **26** (1.18 g, 3.5 mmol) and iron powder (0.78g, 14 mmol) in acetic acid (10 mL) was stirred at 90°C for 2 hrs. The resulting mixture was allowed to cool to ambient

temperature and EtOAc was added. The mixture was filtered, concentrated and the residue chromatographed on silica gel (EtOAc/pet ether) to give **27** as a white solid (600 mg, 56%). <sup>1</sup>H NMR (CDCl<sub>3</sub>): δ 6.81 (d, J=8.1Hz, 1H), 6.74 (d, J=8.1Hz, 1H), 4.85 (br, 2H), 4.13 (t, 2H), 3.58 (t, 2H), 2.38 (m, 2H); MS (ESI) calcd for C<sub>8</sub>H<sub>11</sub>Br<sub>2</sub>N<sub>2</sub>O (m/z): 310.92, found: 311.2.

### **7-Bromo-2,3,4,5-tetrahydropyrido[3,2-b][1,4]oxazepine (28)**

To a stirred solution of **27** (5g, 16 mmol) at 0°C in THF (500 mL) was added NaH (1.29 g, 32 mmol suspended in mineral oil). The resulting mixture was heated and stirred at 100°C for 1h. Saturated NH<sub>4</sub>Cl and water were added and the resulting mixture was extracted with dichloromethane. The combined organic layers were washed with water, then brine, dried over Na<sub>2</sub>SO<sub>4</sub> and concentrated. A second batch of the same scale was run identically as described and the combined crude products were chromatographed (EtOAc/pet ether) to give **28** as a white solid (5.9 g, 80%). <sup>1</sup>H NMR (CDCl<sub>3</sub>): δ 7.00-6.97 (dd, 2H), 4.87 (br, 1H), 4.15 (t, 2H), 3.39 (m, 2H), 2.07 (m, 2H); MS (ESI) calcd for C<sub>8</sub>H<sub>10</sub>BrN<sub>2</sub>O (m/z): 229.00, 231.00, found: 229, 231.

### **7-(3-Chlorophenyl)-2,3,4,5-tetrahydro[3,2-b][1,4]oxazepine (29)**

A mixture of **28** (229 mg, 1 mmol), 3-chlorophenylboronic acid (187 mg, 1.2 mmol), Cs<sub>2</sub>CO<sub>3</sub> (978 mg, 3 mmol) and Pd(dppf)Cl<sub>2</sub> (82 mg, 0.1 mmol) in 1,4-dioxane/H<sub>2</sub>O (10:1, 6 mL) was stirred at 70°C under nitrogen overnight. The reaction mixture was

concentrated. A second batch (**28**, 3.5 g, 15.3 mmol) was run identically as described and the combined crude products were chromatographed on silica gel (EtOAc/pet ether) to give **28** (2.87 g, 68%). <sup>1</sup>H NMR(d<sub>6</sub>-DMSO): δ 8.02 (m, 1H), 7.89 (m, 1H), 7.47-7.37 (m, 2H), 7.26-7.18 (m, 2H), 6.31 (br, 1H), 4.11 (dd, 2H), 3.33 (s, 1H), 3.28 (m, 2H), 1.95 (m, 2H); MS (ESI) calcd for C<sub>14</sub>H<sub>14</sub>ClN<sub>2</sub>O (m/z): 261.08, found: 261.0.

**N-(2-(Azetidin-1-yl)pyridin-4-yl)-7-(3-chlorophenyl)-3,4-dihydropyrido[3,2-b][1,4]oxazepine-5(2H)-carboxamide (6)**

To a mixture of **20** (49 mg, 0.3 mmol) and triethylamine (61 mg, 0.6 mmol) in anhydrous THF (5 mL) was added triphosgene (24 mg, 0.08 mmol). The resulting mixture was stirred at room temperature for 1 hr and **29** (52 mg, 0.2 mmol) was added. The reaction mixture was stirred at reflux for 8 hrs, and a saturated NaHCO<sub>3</sub> solution was added. The reaction mixture was concentrated to dryness and the crude product was purified by prep-TLC to afford **6** (71 mg, 82%). <sup>1</sup>H NMR (CDCl<sub>3</sub>): δ 11.47 (s, 1H), 7.93 (m, 2H), 7.80 (m, 1H), 7.42 (m, 4H), 6.64 (m, 1H), 6.42 (m, 1H), 4.35 (m, 2H), 4.05 (m, 6H), 2.31 (m, 4H); HRMS calcd for C<sub>23</sub>H<sub>23</sub>N<sub>5</sub>O<sub>2</sub>Cl (m/z): 436.1540, found: 436.1541.

**7-(3-Chlorophenyl)-N-(2-(pyrrolidin-1-yl)pyridin-4-yl)-3,4-dihydropyrido[3,2-b][1,4]oxazepine-5(2H)-carboxamide (7)**

To a mixture of **22** (49 mg, 0.3 mmol) and triethylamine (61 mg, 0.6 mmol) in anhydrous THF (5 mL) was added triphosgene (24 mg, 0.08 mmol). The resulting mixture was

stirred at room temperature for 1 hr and **29** (52 mg, 0.2 mmol) was added. The reaction mixture was stirred at reflux for 8 hrs, and then a saturated NaHCO<sub>3</sub> solution was added. The reaction mixture was concentrated to dryness and the crude product was purified by prep-TLC to afford **7** (76 mg, 82%). <sup>1</sup>H NMR (CDCl<sub>3</sub>): δ 11.47 (s, 1H), 7.96-7.92 (m, 2H), 7.80 (d, 1H), 7.48-7.38 (m, 4H), 7.00 (s, 1H), 6.32 (m, 1H), 4.36 (m, 2H), 4.11-3.98 (m, 6H), 2.37-2.27 (m, 4H); HRMS calcd for C<sub>24</sub>H<sub>25</sub>N<sub>5</sub>O<sub>2</sub>Cl (m/z): 450.1697, found: 450.1697.

**7-(3-Chlorophenyl)-N-(6-(2,3-dihydroxypropoxy)pyrazin-2-yl)-3,4-dihydropyrido-[3,2-b][1,4]oxazepine-5(2H)-carboxamide (10)**

To a mixture of **24** (52 mg, 0.23 mmol) and triethylamine (0.3 mL) in anhydrous THF (5 mL) was added triphosgene (28 mg, 0.092 mmol). The reaction mixture was stirred at 60°C for 2-3 hrs. **29** (40 mg, 0.15 mmol) was added to the reaction mixture and stirred again for 18 hrs. Saturated NaHCO<sub>3</sub> solution (5 ml) and dichloromethane (10 ml) were added to the reaction mixture. The organic layer was successively washed with water (10 ml) and brine, dried over Na<sub>2</sub>SO<sub>4</sub> and concentrated. The crude product was purified by prep-TLC (EtOAc/pet ether) to afford **30**, which was taken up in THF (5 mL) and treated with conc. HCl (0.5 mL). The mixture was stirred at room temperature for 2 hrs. Saturated NaHCO<sub>3</sub> was added and the reaction mixture was extracted with CH<sub>2</sub>Cl<sub>2</sub>. The organic layer was washed successively with water and brine, then dried over Na<sub>2</sub>SO<sub>4</sub>, filtered, and concentrated. The crude product was purified by prep-TLC (EtOAc/pet ether) to afford **10** (42 mg, 58% two steps). <sup>1</sup>H NMR(CDCl<sub>3</sub>): δ 11.88 (br, 1H), 8.92 (s,

1H), 8.14-7.83 (m, 3H), 7.50-7.40 (m, 4H), 4.46-4.35 (m, 4H), 4.14-4.07 (m, 3H), 3.75 (t, 2H), 3.25 (s, 1H), 2.30 (t, 2H); HRMS calcd for C<sub>22</sub>H<sub>23</sub>N<sub>5</sub>O<sub>5</sub>Cl (m/z): 472.1388, found: 472.1389.

### **7-(2-Methylpyridin-4-yl)-2,3,4,5-tetrahydropyrido[3,2-b][1,4]oxazepine (31)**

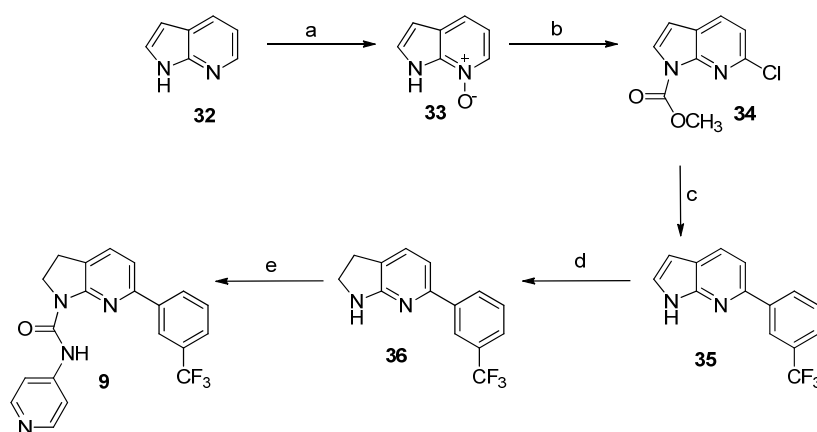
Under a nitrogen atmosphere, a mixture of **28** (687 mg, 3.0 mmol) and (2-methylpyridin-4-yl)boronic acid (575 mg, 4.2 mmol), Pd(dppf)Cl<sub>2</sub> (125 mg, 0.15 mmol) and Cs<sub>2</sub>CO<sub>3</sub> (1.96 g, 6.0 mmol) in 1,4-dioxane (20 mL) was stirred at 95°C for 20 hrs. The resulting mixture was concentrated, purified by flash chromatography (MeOH/CH<sub>2</sub>Cl<sub>2</sub>) to give **30** as a yellow solid (410 mg, 57%). <sup>1</sup>H NMR (CDCl<sub>3</sub>): δ 8.97 (d, J=2.1Hz, 1H), 8.08 (dd, J=2.4, 8.1Hz, 1H), 7.22 (d, J=8.4Hz, 1H), 7.16 (d, J=8.1Hz, 1H), 4.85 (br, 1H), 4.20 (t, 2H), 3.42 (m, 2H), 2.57 (s, 3H), 2.05 (m, 2H); MS (ESI) calcd for C<sub>14</sub>H<sub>16</sub>N<sub>3</sub>O (m/z): 242.13, found: 242.

### **7-(2-Methylpyridin-4-yl)-N-(5-methylthiazol-2-yl)-3,4-dihydropyrido[3,2-b][1,4]oxazepine-5(2H)-carboxamide (8)**

A solution of **31** (40 mg, 0.166 mmol), DIEA (43 mg, 0.33 mmol), and phenyl (4-methylthiazol-2-yl)carbamate (77 mg, 0.33 mmol) in DMSO (2 mL) was stirred at 60°C for 2 hrs. The reaction was quenched with saturated NaHCO<sub>3</sub> solution and diluted with dichloromethane. The reaction mixture was washed successively with water and brine, then dried and concentrated to give a crude product which was purified by prep-TLC to

afford **8** as white solid (25 mg, 39%).  $^1\text{H NMR}$  ( $\text{CDCl}_3$ ):  $\delta$  12.6 (br, 1H), 8.61 (d,  $J=5.4\text{Hz}$ , 1H), 7.87 (m, 1H), 7.60 (m, 1H), 7.58 (d,  $J=6.0\text{Hz}$ , 1H), 7.44 (d,  $J=8.4\text{ Hz}$ , 1H). 6.48 (d,  $J=1.2\text{Hz}$ , 1H), 4.38 (t, 2H), 4.18 (t, 2H), 2.71 (s, 3H), 2.30-2.27 (m, 5H); HRMS calcd for  $\text{C}_{23}\text{H}_{23}\text{N}_5\text{O}_2\text{Cl}$  ( $m/z$ ): 382.1338, found: 382.1338.

*Scheme 6: Preparation of STAC-9*



a) *m*-CPBA,  $\text{CH}_2\text{Cl}_2$ ; b) methylchloroformate, HMDS, THF; c) 3-(trifluoromethyl)phenyl boronic acid,  $\text{Pd}(\text{dppf})\text{Cl}_2$ ,  $\text{Cs}_2\text{CO}_3$ ; d)  $\text{BH}_3\text{-Me}_2\text{S}$ ; e) 4-aminopyridine, triphosgene, TEA, THF.

### 1H-Pyrrolo[2,3]pyridine-7-oxide (33)

To a solution of **32** (20 g, 170 mmol) in dichloromethane (300 mL) was added a suspension of *m*-CPBA (73 g, 430 mmol) in dichloromethane over 30 min at  $0^\circ\text{C}$ . The resulting mixture was allowed to warm to ambient temperature and stirred for 3 hrs. The

mixture was concentrated and re-dissolved in MeOH (200 mL). Saturated aqueous K<sub>2</sub>CO<sub>3</sub> (100 mL) was added and the resulting mixture stirred for 30 min, filtered and concentrated. The residue was triturated in dichloromethane/MeOH (10:1) and the solvent was removed. The residue was chromatographed (dichloromethane/MeOH, 10:1 to 5:1 gradient) to give crude material which was triturated with ether to afford **33** as a yellow solid (9.5 g, 35%) and was used in the next step without further purification. <sup>1</sup>H NMR (CDCl<sub>3</sub>): δ 12.35 (br, 1H), 8.25 (d, 1H), 8.10 (m, H), 8.00 (m, 1H), 7.80 (d, 1H), 7.54 (m, 1H), 7.46 (d, 1H), 7.38 (m, 1H), 7.10 (m, 1H), 6.63 (d,1H).

#### **Methyl-6-chloro-1*H*-pyrrolo[2,3]pyridine-1-carboxylate (34)**

To a solution of **33** (8.9 g, 66 mmol) and HMDS (10.6 mL, 66 mmol) in THF (300 mL) was added methylchloroformate (15.7 g, 166 mmol) dropwise under N<sub>2</sub> at ambient temperature. The reaction mixture was stirred for 1 hr, concentrated and the residue dissolved in EtOAc. The EtOAc solution was washed with saturated aqueous NaHCO<sub>3</sub> (3x) then brine, dried over Na<sub>2</sub>SO<sub>4</sub>, filtered and concentrated. The resulting crude product was chromatographed on silica gel (pet ether/EtOAc, 10:1) to give **34** (3.25 g, 23%) which was used without further purification in the next step. <sup>1</sup>H NMR (CDCl<sub>3</sub>): δ 7.87(d, 1H), 7.76 (d, 1H), 7.29 (d, 1H), 6.59 (d, 1H), 4.14 (s, 3H).

#### **6-(3-(Trifluoromethyl)phenyl)-1*H*-pyrrolo[2,3-*b*]pyridine (35)**

A mixture of **34** (3.25 g, 15.5 mmol), 3-(trifluoromethyl)phenyl boronic acid (5.89 g, 31 mmol), Pd(dppf)Cl<sub>2</sub> (1.26 g, 1.55 mmol) and cesium carbonate (15.1 g, 46 mmol) was stirred at 100°C in 1,4-dioxane/water (10:1, 50 mL) overnight. The reaction mixture was concentrated, re-dissolved in EtOAc, washed with brine and dried over Na<sub>2</sub>SO<sub>4</sub>. Following concentration the crude product was chromatographed (pet ether/EtOAc 20:1) to afford **35** as a white solid (3.62 g, 89%). <sup>1</sup>H NMR (CDCl<sub>3</sub>): δ 8.30 (s, 1H), 8.06 (d, 1H), 7.90 (d, 1H), 7.65-7.55 (m, 3H), 7.38 (m, 1H), 6.55 (m, 1H).

#### **6-(3-(Trifluoromethyl)phenyl)-2,3-dihydro-1H-pyrrolo[2,3-b]pyridine (36)**

To a solution of **35** (3.62 g, 13.8 mmol) in THF (30 mL) was added borane (13.8 mL of 10 M solution in Me<sub>2</sub>S, 138 mmol) and stirred at ambient temperature for 16 hrs. The resulting reaction mixture was concentrated and the residue chromatographed (pet ether/EtOAc 10:1) to give **36** as a yellow solid (0.89 g, 24%). <sup>1</sup>H NMR (CDCl<sub>3</sub>): δ 8.17 (s, 1H), 8.06 (d, *J* = 7.5 Hz, 1H), 7.60-7.49 (m, 2H), 7.33 (d, *J* = 7.5 Hz, 1H), 6.98 (d, *J* = 7.2 Hz, 1H), 4.60 (br, 1H), 3.67 (dt, *J* = 8.1 Hz, 1.2 Hz, 2H), 3.11 (t, *J* = 8.4 Hz, 2H).

#### **N-(Pyridin-4-yl)-6-(3-(trifluoromethyl)phenyl)-2,3-dihydro-1H-pyrrolo[2,3-b]pyridine-1-carboxamide (9)**

To a mixture of 4-amino pyridine (54 mg, 0.19 mmol) in anhydrous THF (3 mL) was added triethylamine (0.5 mL) and triphosgene (68 mg, 0.23 mmol). The resulting mixture was stirred at ambient temperature for 3 hrs. Compound **36** (50 mg, 0.19 mmol) was

added and the mixture was warmed to 60°C and stirred for an additional 18 hrs. Water was added and the resulting aqueous portion was extracted with dichloromethane (3x15 mL). The combined organic extracts were washed with saturated aqueous NaHCO<sub>3</sub>, then with brine, dried over Na<sub>2</sub>SO<sub>4</sub> and concentrated. The crude product was purified by prep-TLC to afford **9** as a white solid (70 mg, 96%). <sup>1</sup>H NMR (CDCl<sub>3</sub>): δ 11.92 (s, 1H), 8.48 (d, *J* = 6.6 Hz, 2H), 8.23 (s, 1H), 8.05 (d, *J* = 8.1 Hz, 1H), 7.75 (d, *J* = 8.4 Hz, 1H), 7.65 (dd, *J* = 15.9 Hz, 7.8 Hz, 2H), 7.56 (d, *J* = 6.3 Hz, 2H), 7.35 (d, *J* = 7.5 Hz, 1H), 4.27 (t, *J* = 9.0 Hz, 2H), 3.21 (t, *J* = 8.4 Hz, 2H); HRMS calcd for C<sub>20</sub>H<sub>16</sub>N<sub>4</sub>O<sub>2</sub>F<sub>3</sub> (m/z): 385.1276, found: 385.1276.

#### Chemical reagents/peptides

In general, all chemicals were purchased from Sigma-Aldrich, with the following exceptions: SIRT1 activating compounds (Sirtris, a GSK company), resveratrol (Orchid Pharmaceuticals), and EX-527 (Tocris). OAcADPr was synthesized by Sirtris, a GSK company. With the exception of Ac-RSGK<sup>TFA</sup>-V-Nle-R-NH<sub>2</sub> (TFA-ACS2 peptide) and Trp 5-mer peptide (Biopeptide), all peptides were custom synthesized by Peptide 2.0 at ≥90% purity, and their sequences may be found below:

FdL-p53	Ac-RHKK(Ac)-AMC
Trp 5-mer	Ac-RHKK(Ac)W-NH <sub>2</sub>
H3-K9 (s)	Ac-TARK(Ac)STG-NH <sub>2</sub>
H3-K9 (l)	Ac-ARTKQTARK(Ac)STGGKAPRKQLATKAA-NH <sub>2</sub>
H3-K9-AMC	Ac-ARTKQTARK(Ac)-AMC
H3-K9-5-AMC	Ac-ARTKQTARK(Ac)STGGK-AMC
H3-K9-9-AMC	Ac-ARTKQTARK(Ac)STGGKAPRK-AMC
H3-K9-17-AMC	Ac-ARTKQTARK(Ac)STGGKAPRKQLATKAAR-AMC
H3-K9(pS10)	Ac-ARTKQTARK(Ac)S(P)TGGKAPRKQLATKAA-NH <sub>2</sub>
p53d	Ac-EEKGQSTSSHSK(Ac)-Nle-STEGAE- NH <sub>2</sub>
p53d(W)	Ac-EEKGQSTSSHSK(Ac)-Nle-STEGWEE-NH <sub>2</sub>
p53d(WAW)	Ac-EEKGQSTSSHSK(Ac)-Nle-STEGWAWEE-NH <sub>2</sub>

p53d(WWF)	Ac-EEKGQSTSSHSK(Ac)-Nle-STEGWWFEE-NH <sub>2</sub>
p53d(WWW)	Ac-EEKGQSTSSHSK(Ac)-Nle-STEGWWWEE-NH <sub>2</sub>
β-catenin-K19	Ac-MAMEPDRK(Ac)AAVSHWQ-NH <sub>2</sub>
FOXO3a-K290	Ac-DSPSQLSK(Ac)WPGSPTS-NH <sub>2</sub>
H3-K56	Ac-EIRRYQK(Ac)STELLI- NH <sub>2</sub>
NFκB-K310	Ac-KRKRTYETFK(Ac)SIMKKSPFS-NH <sub>2</sub>
Smad7-K70	Ac-GKAVRGAK(Ac)GHHHPHP- NH <sub>2</sub>
LKB1-K48	Ac-RRKRAKLIGK(Ac)YLMGDLL- NH <sub>2</sub>
mPGC1α-K778	Ac-SDDDFPASTKSK(Ac)YDSLDFDS-NH <sub>2</sub>
mFOXO3a-K242	Ac-IINPDGGK(Ac)SGKAPRR-NH <sub>2</sub>
eIF2α-K141	Ac-TAWVFDDK(Ac)YKRPGYG-NH <sub>2</sub>
HDAC1-K74	Ac-HSDDYIK(Ac)FLRSIR-NH <sub>2</sub>
HP1α-K40	Ac-QVEYLLK(Ac)WKGFSSE-NH <sub>2</sub>
MTL5-K40	Ac-IGLKAPVK(Ac)YEEDEFH-NH <sub>2</sub>
PPIA-K82	Ac-GKSIYGEK(Ac)FEDENFI-NH <sub>2</sub>
mPGC1α -K778 mutant peptides	Identical to the mPGC1a-K778 peptide, with the indicated modifications.
FOXO3a-K290 mutant peptides	Identical to the FOXO3a-K290 peptide, with the indicated modifications.
mFOXO3a-K242 mutant peptides	Identical to the mFOXO3a-K242 peptide, with the indicated modifications.

### Plasmids/mutagenesis

The constructs used for expression of human SIRT1 and *S. cerevisiae* PNC1, pHEX-SIRT1 and pET28a-His-PNC1, have been previously described (3, 13). New expression constructs were generated using standard cloning strategies, and verified by DNA sequencing. Constructs encoding truncations of human SIRT1 were cloned in between the *Nde*I and *Xho*I sites of pET28b in frame with an N-terminal His tag. Full length SIRT1 cDNA was cloned into pEGFP-N1 using *Sac*I to yield a SIRT1-GFP fusion construct. Site-directed mutagenesis of SIRT1 constructs to produce SIRT1-E230K (or mSIRT1-E222K) was performed using the Quickchange II XL Site Directed Mutagenesis kit (Stratagene). Mouse wild-type mSIRT1 and mSIRT1-E222K were synthesized by Iridium Biosciences. A Kozak sequence (5'CCACC'3) was added 5' to the initial ATG,

and the resultant construct was subcloned into the MCS of the CMV-based vector pVQAd to generate VqAd-SIRT and VqAd-SIRT1-E222K (ViraQuest).

### Protein expression and purification

Plasmids encoding full-length and mutant/truncated versions of His-SIRT1 and His-Pnc1p were transformed into BL21 or BL21 (DE3) bacteria, respectively, and grown at 37°C until an O.D. of 0.6-0.8 was reached. Protein expression was induced by addition of 1 mM IPTG, followed by an additional 16-20 hrs of culturing at 18°C. Next, bacteria were harvested by centrifugation and resuspended in His-tag lysis buffer (1% Triton-X, 50 mM Tris, pH 8, 150 mM NaCl, 20 mM Imidazole, and 3 mM BME) supplemented with protease inhibitors (Roche) for 30 minutes on ice. Samples were then sonicated 5X to disrupt the cell wall, and centrifuged to remove insoluble debris. Clarified supernatants were added to Ni-NTA agarose beads (3 mL / 4 L induction) and gently rotated for 2-3 hrs at 4°C. Following removal of the supernatant, beads were washed 3X with lysis buffer. The protein was eluted from the beads using a Poly-prep column (Biorad) with Elution buffer (50 mM Tris pH 7.4 or 8.0, 250 mM Imidazole, 3 mM BME). Glycerol was added in a 1:1 ratio to the eluted protein solutions prior to storage at -20 °C.

Additional His-SIRT1-wild-type, His-SIRT1-E230K, and His-SIRT1-E230A, were expressed and purified in a similar manner. These protein samples were also purified by Ceramic Hydroxyapatite chromatography (Bio-Rad) in a buffer containing 20 mM HEPES pH 6.8, 100 mM NaCl, 0.1 mM TCEP with a gradient elution from 25 mM PBS to 200 mM PBS. Subsequently, protein samples were concentrated and further purified by size exclusion chromatography using a Superdex 200 26/60 column (GE

Lifesciences) in buffer containing 50 mM Tris HCl pH 7.5, 300 mM NaCl, 0.1 mM TCEP. Enzyme concentrations were determined by a Bradford assay using BSA as a standard. Final protein purity for these samples, as assessed by gel densitometry for WT, E230K, and E230A, was 90%, 95%, and 85%, respectively. Proteins were confirmed either by LC/MS or protein peptide mapping.

#### Screening for mutations affecting SIRT1 activation by resveratrol

Following hydroxylamine mutagenesis, cultures for the +/- resveratrol mutant screening were grown in deep well (1 mL) 96-well plates and induced with 1 mM IPTG at 30°C for 2.5 hr. Bacterial pellets were lysed with B-PER reagent (Pierce) and the crude, clarified extract (10  $\mu$ L) was assayed using the Biomol assay (see below), 20 min., 37°C reactions, +/- 100  $\mu$ M resveratrol. The single-lysine FdL substrate (Enzo Life Sciences, formerly BIOMOL Cat. #KI-104) was used at a concentration of 25  $\mu$ M and the concentration of  $\beta$ -NAD<sup>+</sup> was 500  $\mu$ M. A total of approximately 2208 clones were tested.

Of the 2208 clones tested, eight candidate clones with low +resv/-resv. activity ratios were identified and sequenced. Of these, two displayed actual coding changes, corresponding to amino acid substitutions E230K and V392D. Secondary characterization of these proteins revealed that SIRT1-E230K was indeed unable to be activated by resveratrol, but that SIRT1-V392D could be activated by resveratrol, and was therefore likely a false positive.

#### BIOMOL assay

The AMC-based Fluor-de-Lys assay was performed in accordance with the manufacturer's instructions (Enzo Life Sciences, formerly BIOMOL Cat. #KI-104) using approximately 1  $\mu\text{g}$  of SIRT1 per reaction, and the indicated amounts of  $\beta$ -NAD and FdL-p53 substrate. For reactions examining fold-activation by STACs, the concentrations of  $\beta$ -NAD and substrate were 75  $\mu\text{M}$  and 25  $\mu\text{M}$ , respectively. For determination of  $K_M$  FdL-p53 the concentration of  $\beta$ -NAD was 5 mM, and for  $K_M$   $\beta$ -NAD determination the FdL-p53 concentration was 400  $\mu\text{M}$ . Reactions were allowed to proceed for an incubation period of 1 hr at 37°C prior to addition of developing reagent. All reactions were normalized to control reactions in the absence of  $\beta$ -NAD ( $F_{\text{final}} = F_{+\text{NAD}} - F_{-\text{NAD}}$ ).

#### PNC1-OPT assay

In general, deacetylation reactions were performed in Eppendorf tubes using 1-2  $\mu\text{g}$  of recombinant SIRT1 and 2-4  $\mu\text{g}$  of recombinant *Saccharomyces cerevisiae* Pnc1p per reaction in 1X Gibco PBS (pH 7.4) supplemented with 1 mM DTT and the appropriate amounts of  $\beta$ -NAD and acetyl-substrate. Due to variations in the specific activity of different SIRT1 preparations, the enzyme concentration was adjusted for certain experiments ( $< 1 \mu\text{g}$  in some cases). For reactions examining fold activation by STACs, the concentrations of  $\beta$ -NAD and substrate were 75  $\mu\text{M}$  and 10  $\mu\text{M}$ . For experiments assessing the effects of inhibitors, the concentrations of  $\beta$ -NAD and substrate were 200  $\mu\text{M}$  and 100  $\mu\text{M}$ , respectively.

For determinations of  $K_M$  H3K9 peptide and  $K_M$   $\beta$ -NAD<sup>+</sup> the concentrations of  $\beta$ -NAD and H3K9 peptide were 1.5 mM and 300  $\mu\text{M}$ , respectively. The final volume of each reaction was 100  $\mu\text{L}$ . Reactions were allowed to proceed for 1 hr at 37°C.

Subsequently, 100  $\mu$ L of pre-warmed OPT Developer mix [10 mM ortho-phthalaldehyde, 10 mM DTT in 30% EtOH/70% Gibco PBS (pH 7.4)] was added to each reaction under dim light, mixed, and allowed to incubate for 1 hr at room temperature in the dark. Samples were then transferred to a 96-well plate for reading. Measurements were performed on a Victor<sup>3</sup> fluorometer with excitation and emission filters set to 420 nm and 460 nm, respectively. An early version of the assay employed BIOMOL assay buffer and a developer reagent consisting of 10 mM ortho-phthalaldehyde and 10 mM DTT in 100% EtOH. For each sample, background control reactions lacking  $\beta$ -NAD, or lacking enzyme in certain instances, were performed. Final measurements were calculated as follows:  $F_{\text{corrected}} = F_{+\text{NAD}} - F_{-\text{NADcontrol}}$ . Standard curves were generated by incubating fixed amounts of nicotinamide in assay buffer with *S. cerevisiae* Pnc1p as described above, followed by development of the reaction as outlined above.

#### O-Acetyl ADP ribose mass spectrometry assay (OAcADPR assay)

Mass spectrometry parameters were optimized using a direct infusion of OAADPr in 1:1 ethanol:water containing 0.1% formic acid and infused at 10  $\mu$ L/min. The following mass spectrometry parameters were set: curtain gas 20, probe temperature 550°C, ion source gas 1 50, ion source gas 2 50, interface heater on, collision gas 10, ion source voltage -3,800 V, declustering potential -85 V, entrance potential -10 V, collision energy -37 V, and collision exit potential -20 V. Negative MRM mode was used monitoring the transition 600.1/345.9 for the parent /daughter ion under low-resolution conditions.

Quenched reaction samples were analyzed on an Agilent RapidFire 200 High-Throughput Mass Spectrometry System (Agilent, Wakefield, MA) coupled to an AB Sciex API 4000 mass spectrometer fitted with an electrospray ionization source. The RapidFire system applies 10  $\mu$ L of each sample to a solid phase extraction (SPE) cartridge packed with a cross-linked diol HILIC resin material (200  $\text{\AA}$ , 5  $\mu$ m, Phenomenex, Torrance, CA). Samples were aspirated for 250 ms using the Rapid-Fire system and absorbed onto the SPE cartridge with Buffer A (90:10 acetonitrile:H<sub>2</sub>O with 0.1 mM NH<sub>4</sub>Ac and 0.2% formic acid) for 3 sec and eluted in Buffer B (60:40 acetonitrile: H<sub>2</sub>O supplemented with 1.6 mM NH<sub>4</sub>Ac) for 5 sec. The system was re-equilibrated in Buffer A for 500 ms. Peak data were integrated using RapidFire Integrator software (Agilent, Santa Clara, CA).

Deacetylation reactions were performed at 25°C in reaction buffer (50 mM HEPES, pH 7.5, 150 mM NaCl, 1 mM DTT, and 1% DMSO) in the presence of 0.05% BSA. Time points were taken by quenching the SIRT1 reaction with a stop buffer to give a final concentration of 1% formic acid and 5 mM nicotinamide. Test compounds were pre-incubated with enzyme for 20 minutes before starting the reaction with substrates. Initial velocities vs. SIRT1 concentration were tested using the following parameters: 2  $\mu$ M Trp 5-mer with 8  $\mu$ M NAD<sup>+</sup> and varying SIRT1. The K<sub>M</sub> of the Trp 5-mer was determined using an NAD<sup>+</sup> concentration of 5 mM and 2.5 nM SIRT1.

Activation assays presented in Figure 1 employed enzyme, peptide substrate, and NAD<sup>+</sup> concentrations of 200 nM, 10  $\mu$ M, and 75  $\mu$ M, respectively.

For measurement of K<sub>M FOXO3a</sub>, 5 nM SIRT1 enzyme and 4 mM NAD<sup>+</sup> were used. Initial velocities were measured from reaction time courses at each substrate

concentration. Product counts were converted to nM product using a standard curve of OAcADPR in assay buffer with 0.05 % BSA and 4 mM NAD. Addition of 5  $\mu$ M STAC-2 had no effect on the OAcADPR standard curve (data not shown).

For assays involving inhibition of WT, E230K, and E230A SIRT1, the concentration of Trp 5-mer peptide used was 2  $\mu$ M, 4  $\mu$ M, and 4  $\mu$ M for WT, E230K, and E230A respectively and the NAD<sup>+</sup> concentration was 80  $\mu$ M. Enzymes were tested at 5 nM with a 30 min assay time.

STAC activation assays using the Trp 5-mer peptide used subsaturating substrate concentrations. The Trp 5-mer peptide was tested at 0.2, 0.4, and 0.4  $\mu$ M for WT, E230K, and E230A respectively and the NAD<sup>+</sup> concentration was 8  $\mu$ M. Enzyme concentration was 5 nM. For the activation screen, a chemically diverse set of 117 compounds from the Sirtris activator library was tested in duplicate at 25  $\mu$ M each. The dose-response curves were done in triplicate and the data were described by eq 1

$$\frac{v_x}{v_o} = 1 + \frac{RV_{\max} - 1}{1 + \frac{EC_{50}}{[X]_o}} \quad \text{(Eq. 1)}$$

where  $v_x/v_o$  is the relative rate of reaction in the presence ( $v_x$ ) versus absence ( $v_o$ ) of activator (X),  $RV_{\max}$  is the maximal relative velocity at infinite activator concentration, and  $EC_{50}$  is the concentration of activator producing half of the maximal activation. As saturation of activation was not well determined, the  $EC_{1.5}$  values (concentration of activator required to produce 150% activity) were calculated and the maximum observed activation was reported in place of  $RV_{\max}$ . Reactions were allowed to proceed for 30 min.

### PNC1/GDH assay

The PNC1/GDH assay was performed as previously described (31) using the same reaction buffer as the OAcADPR assay and all reactions were run at 25°C using 50 nM SIRT1 enzyme.  $K_M$  determinations for wild-type SIRT1, E230K and E230A were performed for the Trp 5-mer in the presence of 5 mM  $NAD^+$ .  $K_M$  determinations for  $NAD^+$  were performed in the presence of 200  $\mu$ M Trp 5-mer.

### Isothermal titration calorimetry

ITC experiments were performed using an iTC200 system (MicroCal) at 26°C in reaction buffer (137 mM NaCl, 2.7 mM KCl, 1 mM  $MgCl_2$ , 2 mM TCEP, 5% v/v glycerol and 50 mM HEPES-NaOH, pH 7.3). hSIRT1(183-664) was purified and dialyzed against the buffer, centrifuged, and degassed before the experiment. Titrating ligand into protein yielded a large dilution heat background. A titration of protein into ligand was therefore performed to minimize background. The compounds were dissolved in the final dialysis buffer and their pH values were adjusted to match that of the protein solution. In a typical binding experiment to characterize the STAC/hSIRT1(183-664) interaction performed on the iTC200 system, 100  $\mu$ M enzyme was injected in 20 aliquots of 2  $\mu$ l (except the first injection, which was 0.5  $\mu$ l) into a 0.202 ml sample cell containing 10  $\mu$ M STAC (13).

### Circular dichroism measurements

SIRT1 and SIRT1-E230K proteins were prepared as described above and purified by size exclusion chromatography on a Superdex 200 prep grade column using buffer

consisting of 20 mM Tris pH 8.5, and 150 mM NaCl. Standard spectra were recorded at typical protein concentrations of ~0.1 mg/mL on a Jasco J-815 instrument at room temperature in pH 8.5 buffer containing 5 mM Tris and 50 mM Na<sub>2</sub>SO<sub>4</sub>. A 1 mm path length cell was used. Thermal denaturation readings were taken at intervals of 2°C between 25°C and 95°C.

#### Thermal shift assay

The thermal shift assay (TSA) was done on an Applied Biosystems ViiA 7 Real-time PCR system. Briefly, full-length SIRT1 wild-type or E230K mutant was mixed with Sypro Orange Dye to reach a final concentration of 1 μM protein and 2.5x of the temperature-sensitive dye Sypro Orange in 96-well PCR plate. The sample was subjected to temperature denaturation from 25°C to 95°C with Sypro Orange fluorescence being monitored simultaneously.

#### Hydrogen-deuterium exchange mass spectrometry

*On-exchange experiment of SIRT1.* H/D exchange reactions followed by pepsin digestion, desalting, HPLC separation, and MS analysis were carried out using a fully automated system. Briefly, on-exchange reaction was initiated by mixing 8 μL of 2.1 mg/mL (25 μM) SIRT1 and 32 μL of 50 mM phosphate, 150 mM NaCl, pH<sub>read</sub> 7.0 in D<sub>2</sub>O. The reaction mixture was incubated at 0°C for 15, 50, 150, 500, 1,500, or 5,000 s. The on-exchanged solution was quenched by the addition of 20 μL of 1.6 M guanidine hydrochloride (GuHCl), 0.8% formic acid, pH 2.3 and then immediately analyzed.

*Fully deuterated experiment of SIRT1.* The fully deuterated sample was prepared by incubating the mixture of 20  $\mu\text{L}$  of 2.1 mg/mL (25  $\mu\text{M}$ ) SIRT1 with 80  $\mu\text{L}$  of 100 mM TCEP in  $\text{D}_2\text{O}$ , pH 2.5 at 60°C for 3 hrs. After the incubation and cooling down to 0°C, the sample was quenched identically to an on-exchanged solution.

*General protein process for standard HDX sample.* The quenched solution was pumped over a pepsin column (104  $\mu\text{L}$  bed volume) filled with porcine pepsin (Sigma) immobilized on Poros 20 AL media (Applied Biosystems) per the manufacturer's instructions with 0.05% aqueous TFA (200  $\mu\text{L}/\text{min}$ ) for two min. The digested fragments were temporarily collected on a reverse phase trap column (4  $\mu\text{L}$  bed volume) and desalted. The peptide fragments were then eluted from the trap column and separated by C18 column (BioBacis-18; Thermo Scientific, San Jose, CA) with a linear gradient of 13% solvent B to 40% solvent B over 23 min (solvent A, 0.05% TFA in water; solvent B, 95% acetonitrile, 5% buffer A; flow rate 10  $\mu\text{L}/\text{min}$ ). Mass spectrometric analyses were carried out using a LTQ OrbiTrap XL mass spectrometer (Thermo Scientific, San Jose, CA) with capillary temperature at 200°C.

*Determination of deuteration level of each peptide after on exchange reaction.* The centroids of peptide isotopic envelopes were measured using the in-house-developed program in collaboration with Sierra Analytics. Corrections for back-exchange during the protein processing step were made employing the following standard equation:

$$\text{Deuteration Level (\%)} = \frac{m(\text{P}) - m(\text{N})}{m(\text{F}) - m(\text{N})} \times 100 \quad (\text{Eq.2})$$

where  $m(\text{P})$ ,  $m(\text{N})$ , and  $m(\text{F})$  are the centroid value of partially deuterated (on-exchanged) peptide, non-deuterated peptide, and fully deuterated peptide, respectively.

### Adenoviral Production

Adenoviral production was carried out by ViraQuest Inc. Vectors were confirmed by sequencing and viral particles were purified by two rounds of CsCl gradient centrifugation, dialyzed, and stored at  $\sim 10^{12}$  particles/mL in a TRIS buffer with sucrose as the cryoprotectant.

### MEF cell culture, treatments and adenoviral infections

WT and SIRT1 KO MEFs (a kind gift from Dr. Michael McBurney, University of Ottawa) were cultured in high glucose Dulbecco's modified eagle medium (DMEM) (Invitrogen) supplemented with 10% FBS (Invitrogen) and a mix of antibiotic and antimycotic agents (Invitrogen). The cells were infected with empty, SIRT1-WT and SIRT1-E230K adenoviruses at an MOI of 2, and cells were given fresh media 24 hrs later. Cells were treated with either vehicle (0.0001% DMSO), resveratrol (25  $\mu$ M), STAC-4 (1  $\mu$ M), or STAC-1 (1  $\mu$ M) for an additional 24 hrs. For the AMPK activation assay MEFs were treated with the indicated STAC (doses listed above) for 24 hrs.

### Generation of primary myoblasts from Cre-ERT2 x SIRT1<sup>flox $\Delta$ E4/flox $\Delta$ E4</sup> mice and myoblast treatments

Skeletal muscle was dissected from the hind limb muscles of 4-month-old C57BL/6J mice carrying both the Cre-ERT2 and the SIRT1<sup>flox $\Delta$ E4/flox $\Delta$ E4</sup> alleles (Cre-ERT2 x SIRT1<sup>flox $\Delta$ E4/flox $\Delta$ E4</sup>). Tissue was collected into a tube filled with phosphate buffered saline (CellGrow). Initially, the tissue was minced and dissociated enzymatically using a solution of collagenase (Sigma-Aldrich), Dispase (Roche) and calcium chloride

for 2 hrs at 37°C. Extracts were mechanically triturated and the resulting cell suspension was passed through a cell strainer. The filtrate was then centrifuged at 400 xg for 5 min, suspended in DMEM and transferred to a culture flask for 30 min. The non-adherent cells were removed from the flask and pelleted by centrifugation at 300 xg for 5 min. The pellet was suspended in growth media (F-10 nutrient mix supplemented with 2.5 ng/mL bFGF, 10 ng/mL EGF, 1 µg/mL insulin, 0.5 mg/mL fetuin, 0.4 µg/mL dexamethasone, antibiotic and antimycotic mix and 20% FBS) and plated in collagen coated culture flasks. To induce the excision of exon 4 of SIRT1 the cells were treated with 250 nM 4-hydroxytamoxifen (Sigma-Aldrich), or vehicle (0.001% ethanol), for 48 h, then infected with adenovirus and treated with STACs as described above for MEFs. Cells were then harvested and RNA was collected using an RNeasy kit (Qiagen). Quantification of RNA was performed using the NanoDrop 1000 spectrophotometer (Thermo Scientific). cDNA was synthesized with the iSCRIP cDNA synthesis kit (BioRad) using 800 ng of RNA. This cDNA was used to perform PCR to confirm exon 4 excision and to check the efficiency of the reconstitution with SIRT1 WT and SIRT1 E230K, using primers that target the junction between Exon3 and Exon4 of SIRT1. 18S was used as control. The following primers were used: SIRT1E3-4: Fw TGGATGATATGACGCTGTGGCAGA, Rv AAGTCAGGAATCCCACAGGAGACA; 18S: Fw cggtaccacatccaaggaa, Rv gctggaattaccgcgct. All animals were housed according to the guidelines of the Harvard Institutional Animal Care and Use Committee.

### ATP Content

Cellular ATP content in both MEFs and primary myoblasts was measured with a commercial kit according to the manufacturer's instructions (Roche), as previously described (27).

### Mitochondrial mass

Primary myoblasts and MEFs were incubated in DMEM containing 10 nM of N-nonyl acridine orange (NAO) (Invitrogen), or 10 nM Mitotracker Deep Red (Invitrogen) for 30 min at 37°C in the dark, respectively. The cells were then trypsinized and resuspended in DMEM without NAO, or Mitotracker Deep Red. The NAO/ Mitotracker Deep Red fluorescence intensity was determined by flow cytometry on the FACSCalibur (BD Biosciences).

### Mitochondrial DNA

Total DNA was extracted using a DNease kit (Qiagen), according to the manufacturer's instructions. Quantitative RT-PCR reactions were performed using 1 μM of primers and LightCycler® 480 SYBR Green Master (Roche) on a LightCycler® 480 detection system (Roche). Calculations were performed by a comparative method ( $2^{-\Delta CT}$ ). mtDNA was amplified using primers specific for the mitochondrial cytochrome c oxidase subunit 2 (COX2) gene and normalized to genomic DNA by amplification of the ribosomal protein s18 (RSP18) nuclear gene.

RSP18: Fw TGTGTTAGGGGACTGGTGGACA; Rv

CATCACCCACTTACCCCCAAAA. COX2: Fw ATAACCGAGTCGTTCTGCCAAT;

Rv TTTCAGAGCATTGGCCATAGAA

### Immunoblotting

Protein extracts from MEF cells were obtained by lysis in ice-cold buffer (150 mM NaCl, 10 mM Tris HCl (pH 7.4), 1 mM EDTA, 1 mM EGTA, 1 % Triton X-100, 0.5% NP-40) supplemented with a cocktail of protease and phosphatase inhibitors (Roche). Protein content was determined by the Bradford protein assay (Biorad), and 50 µg of protein was run on SDS-PAGE under reducing conditions, then transferred to a polyvinylidene difluoride membrane (Perkin-Elmer). Antibodies were used at the following concentrations: anti-SIRT1 (1:4000; Sigma-Aldrich), anti-β-tubulin, anti-phospho-AMPKα (Thr172) (1:1000; Cell Signaling) and anti-AMPKα (1:1000; Cell Signaling) overnight at 4°C.

### Transient transfection

Transfections were performed using FuGENE HD according to the manufacturer's instructions.

### GFP Imaging

GFP constructs were transiently transfected into cells as described above, and cells were treated with cell permeable Hoechst 33342 stain (Invitrogen) for one hr according to the manufacturer's instructions. Subsequently, cells were washed with

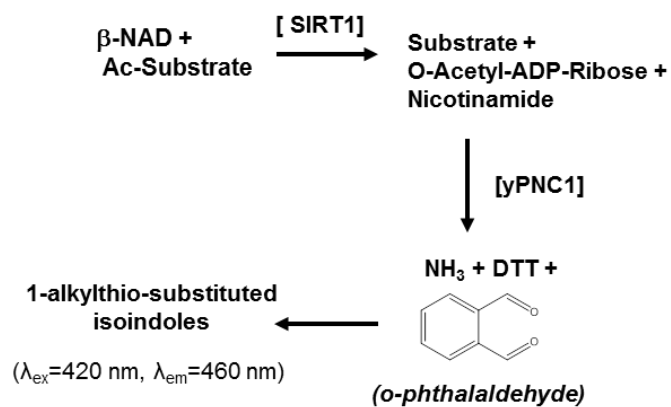
Dulbecco's PBS (Gibco) and switched to normal media for 1 hr prior to being examined using a Nikon TiE fluorescent microscope.

#### Phosphodiesterase (PDE) activity assays

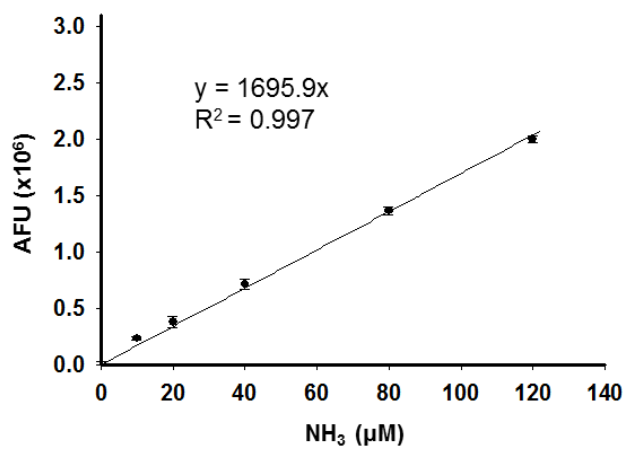
Microfluidic LabChip assays were performed by Caliper Life Sciences (Perkin Elmer) using Caliper LabChip 3000 and 12- sipper LabChip instruments.

Phosphodiesterase-specific inhibitors were used as positive controls for each of the assays.

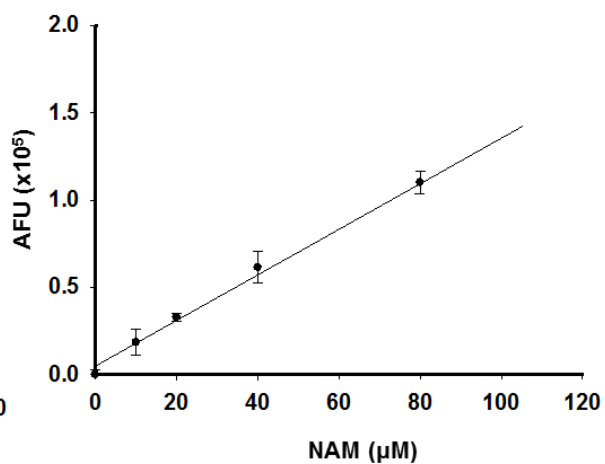
A



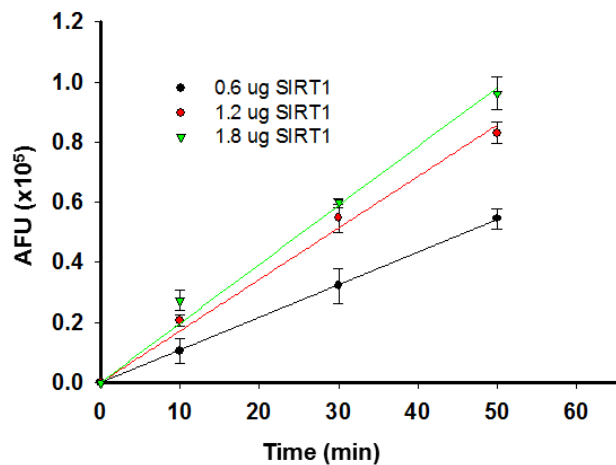
B



C



D



E

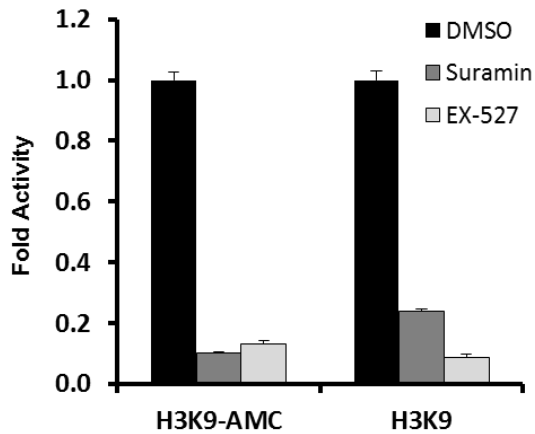
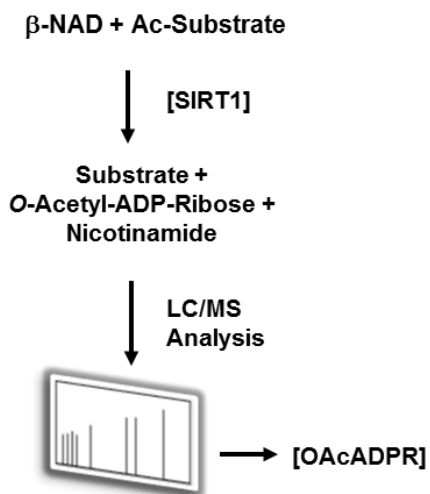
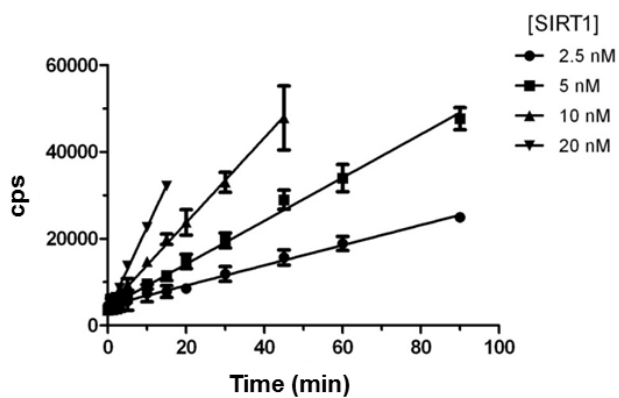


**Fig. S1.** Validation of the PNC1-OPT assay. **A)** Schematic outline of the PNC1-OPT assay. **B)** Standard curve for ammonia detection via reaction with OPT; mean  $\pm$  SD shown (n = 3). **C)** Standard curve for nicotinamide using the PNC1-OPT assay; mean  $\pm$  SD shown (n = 3). **D)** Detection of SIRT1 activity at different time points with different enzyme amounts using H3K9 peptide as substrate (measured after a 10 minute period to allow temperature equilibrium to occur); mean  $\pm$  SEM shown (n = 3). **E)** Inhibition of SIRT1 deacetylase activity on tagged and non-tagged H3K9 peptides; mean + SEM shown (n = 3). EX-527 and suramin were both used at a dose of 10  $\mu$ M.

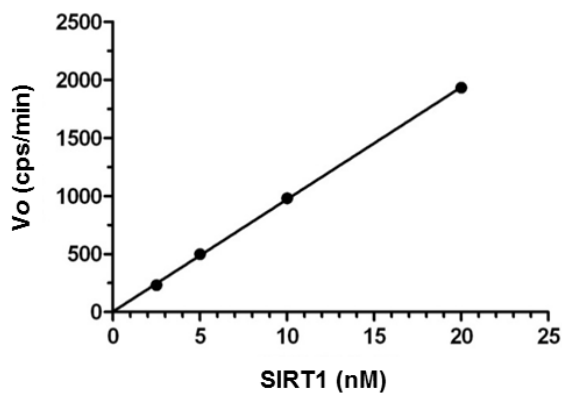
A



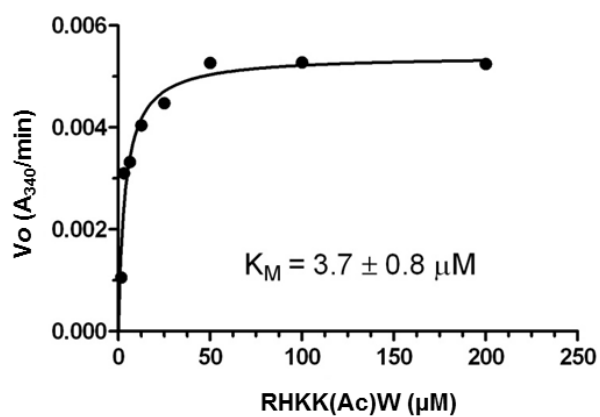
B



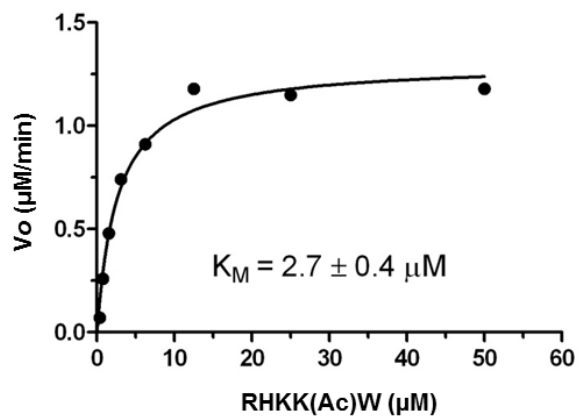
C



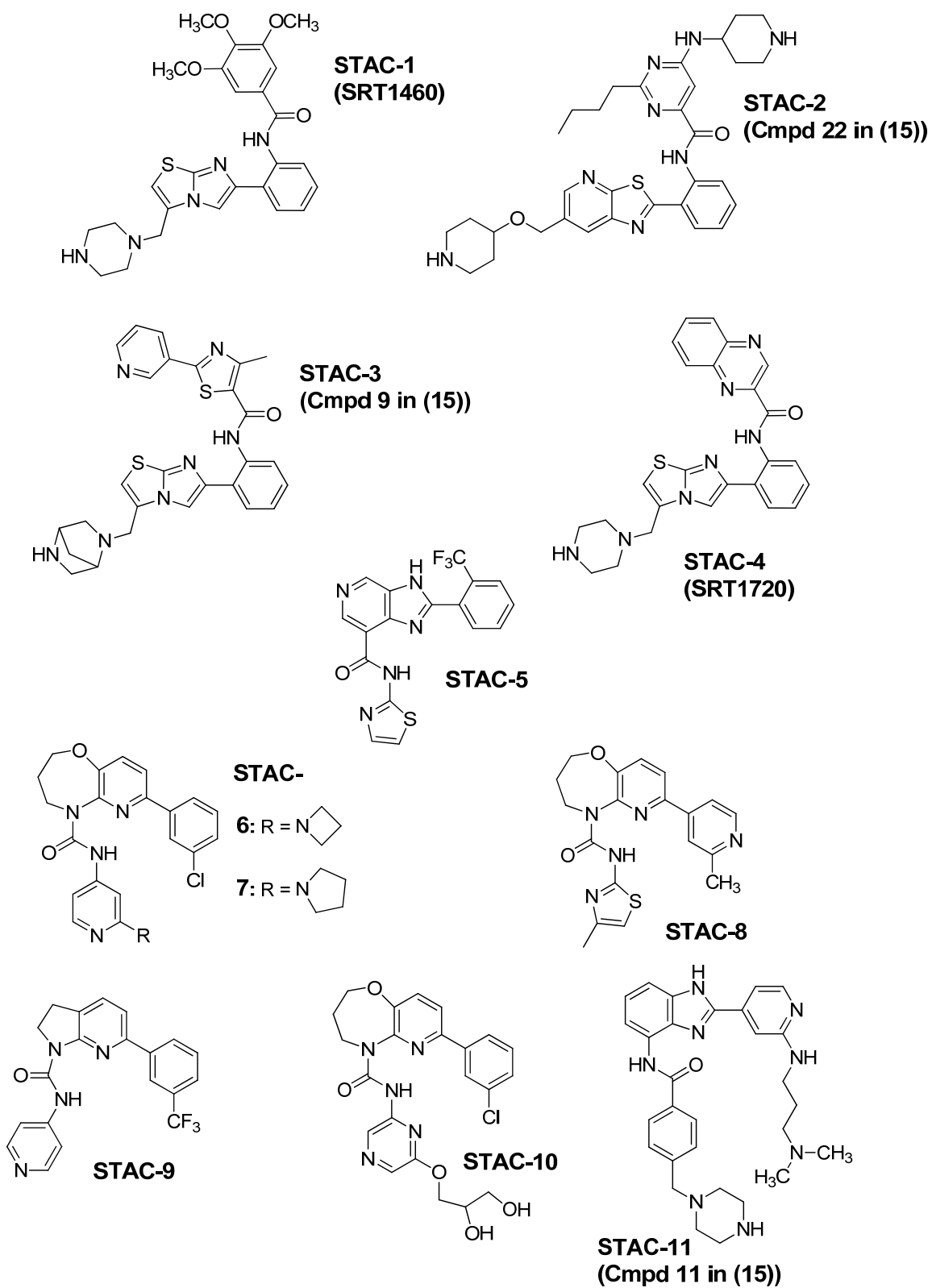
D



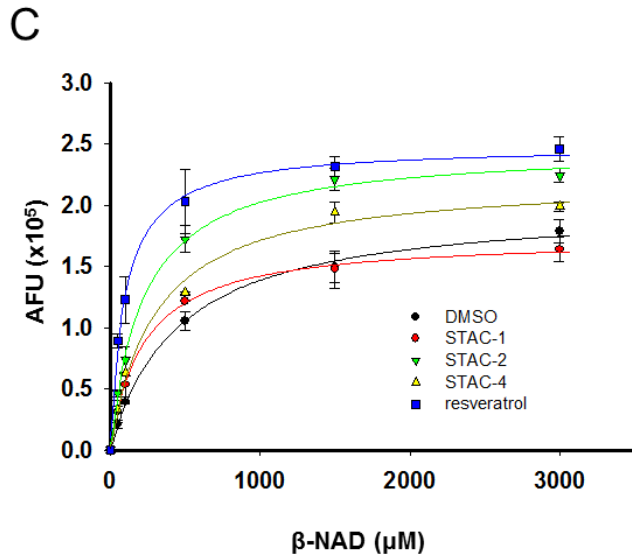
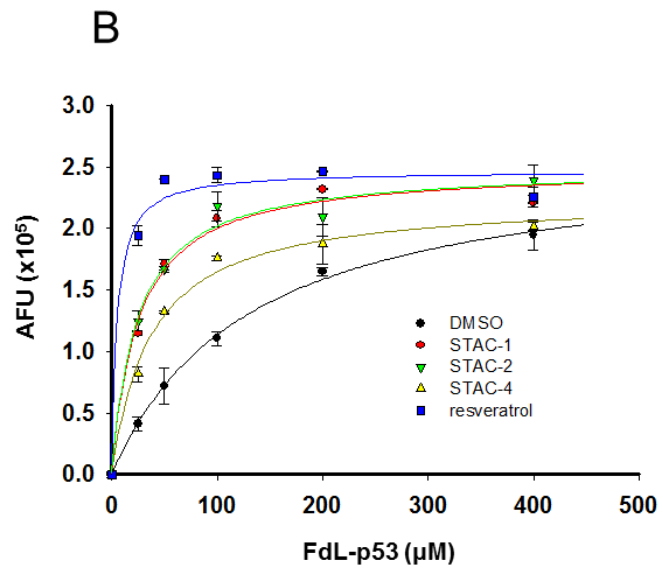
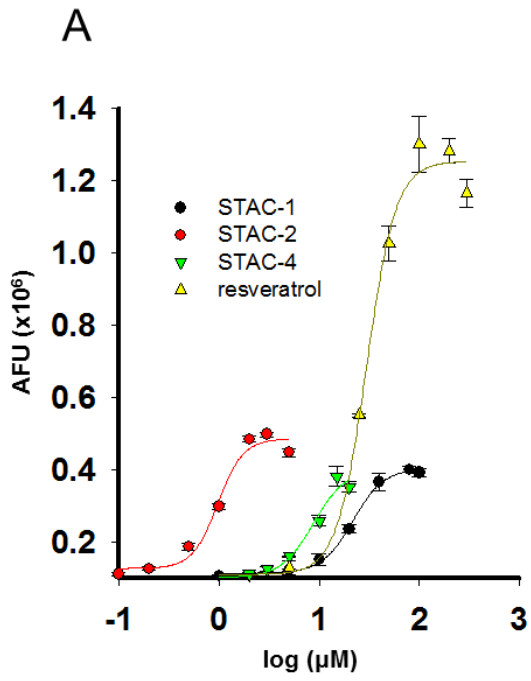
E



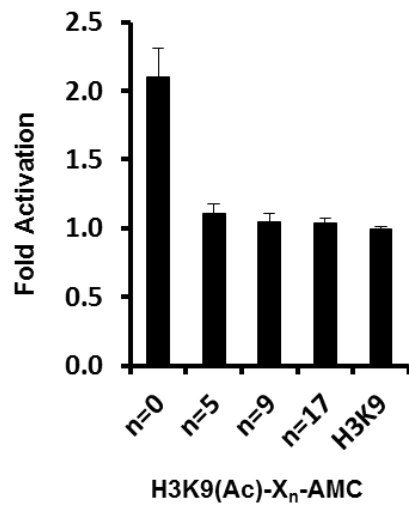
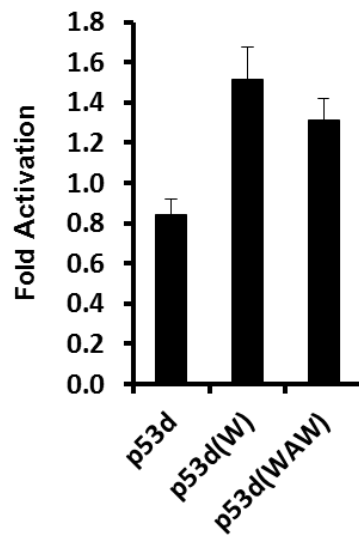
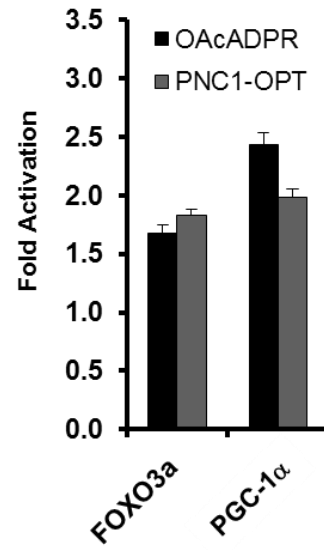
**Fig. S2.** Validation of the OAcADPR assay. **A)** Diagram outlining the OAcADPR assay. **B)** Time courses of deacetylation using the Trp 5-mer substrate and varying amounts of SIRT1; mean  $\pm$  SD shown ( $n = 3$ ). **C)** The dependence of the initial velocity on SIRT1 concentration from A. Comparison of Trp 5-mer  $K_{Ms}$  for SIRT1 determined using either the **D)** PNC1/GDH assay, or **E)** OAcADPR assay.  $K_M$  values are shown  $\pm$  curve-fit errors.



**Fig. S3.** Chemical structures of synthetic SIRT1 activators (STACs).

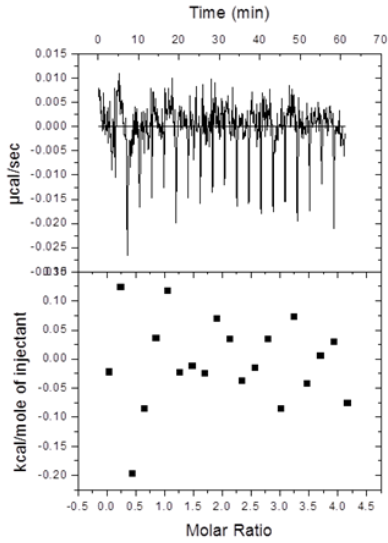


**Fig. S4.** Effects of STACs identified using a TAMRA-based assay in the BIOMOL AMC-based assay. **A)** Dose titration curves for resveratrol and several synthetic STACs; mean  $\pm$  SD shown (n = 3). **B)** Determination of  $K_M$  FdL-p53 for SIRT1 in the presence of the indicated STACs; mean  $\pm$  SD shown (n = 3). **C)** Determination of  $K_M$  NAD<sup>+</sup> for SIRT1 in the presence of the indicated STACs; mean  $\pm$  SD shown (n = 3). For  $K_M$  determination experiments, resveratrol, STAC-1, STAC-2, and STAC-4 were used at doses of 100, 50, 5, and 10  $\mu$ M, respectively.

**A****B****C**

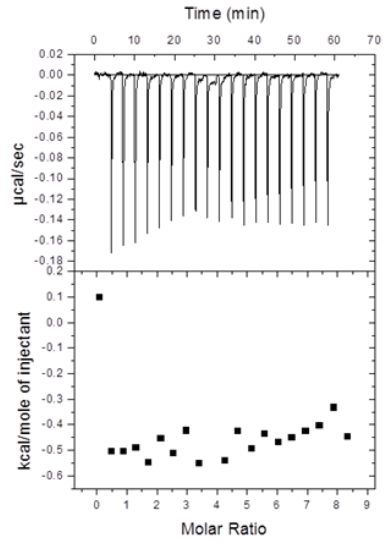
**Fig. S5.** SIRT1 activation by STACs using modified and natural amino acid peptide substrates. **A)** Activation of SIRT1 by STAC-3 on peptides bearing an AMC moiety at the indicated positions using the PNC1-OPT assay; mean + SEM (n = 3). **B)** SIRT1 activation by STAC-3 on peptides containing hydrophobic patches using the PNC1-OPT assay; mean + SEM (n = 3). **C)** Comparison between the fold-activation observed in the PNC1-OPT assay with that observed in the OAcADPR assay on native sequences with STAC-2; mean + SD (n = 3).

**A** Binding of PGC-1 $\alpha$  peptide to STAC-1



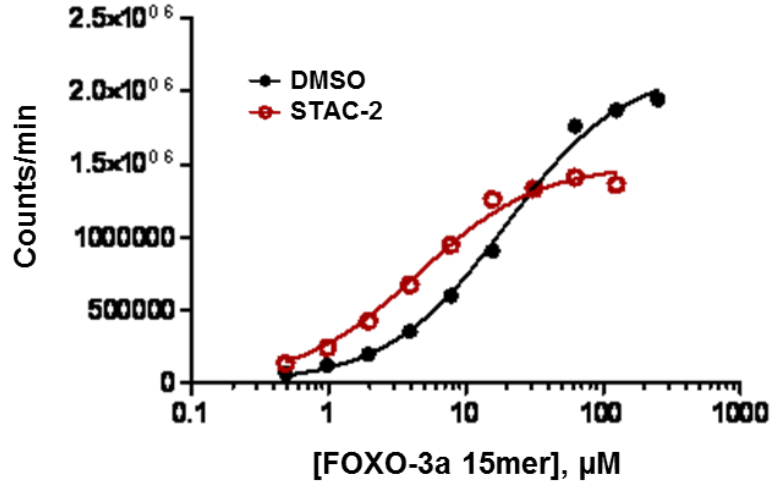
No Binding

**B** Binding of PGC-1 $\alpha$  peptide to STAC-2 (w/1% DMSO)



No Binding

**C**

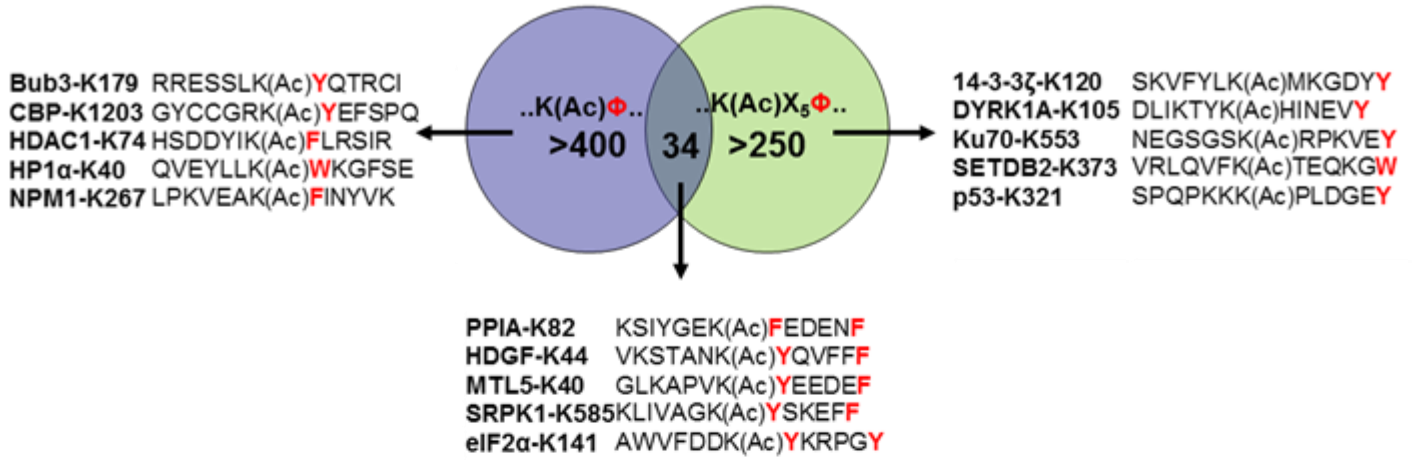


	DMSO	STAC-2 (5 $\mu\text{M}$ )
$V_{\text{max}}$ (counts/min)	$2.16 \pm 0.05 \times 10^6$	$1.50 \pm 0.04 \times 10^6$
$K_M$ ( $\mu\text{M}$ )	$20 \pm 1.5$	$4.5 \pm 0.5$

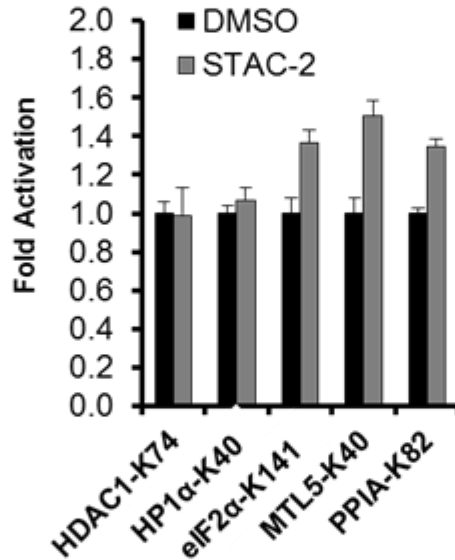
**Fig. S6.** Substrate binding and kinetic mechanism of activation. Assessment of binding between the PGC-1 $\alpha$ -788 peptide and **A)** STAC-1 or **B)** STAC-2 using isothermal titration calorimetry (ITC). **C)** Determination of  $K_M$  FOXO3a in the presence or absence of 5  $\mu$ M STAC-2 using the OAcADPR assay (n = 3). Kinetic parameters are shown in the table below.

# A Potential STAC target sequences

$\Phi = \{W, Y, F\}$



## B



## C

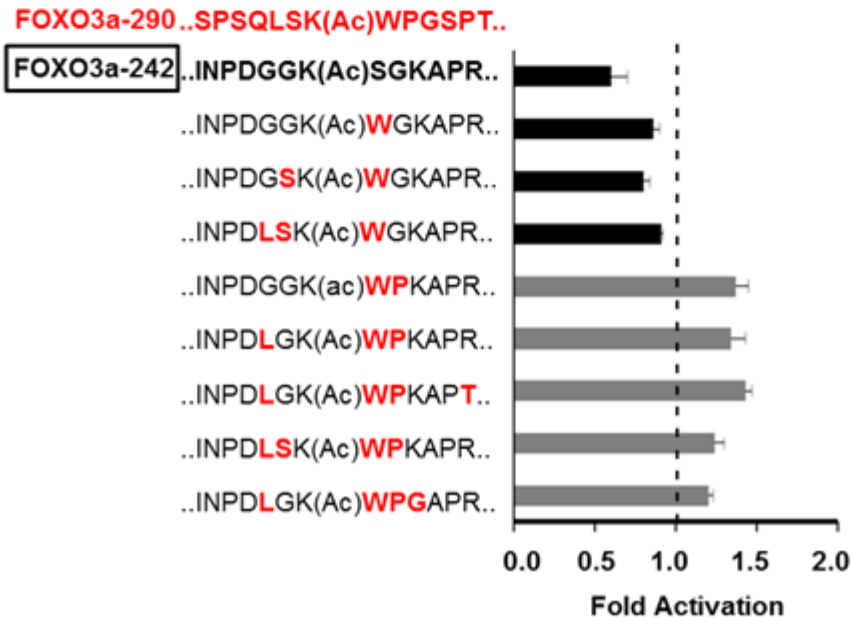
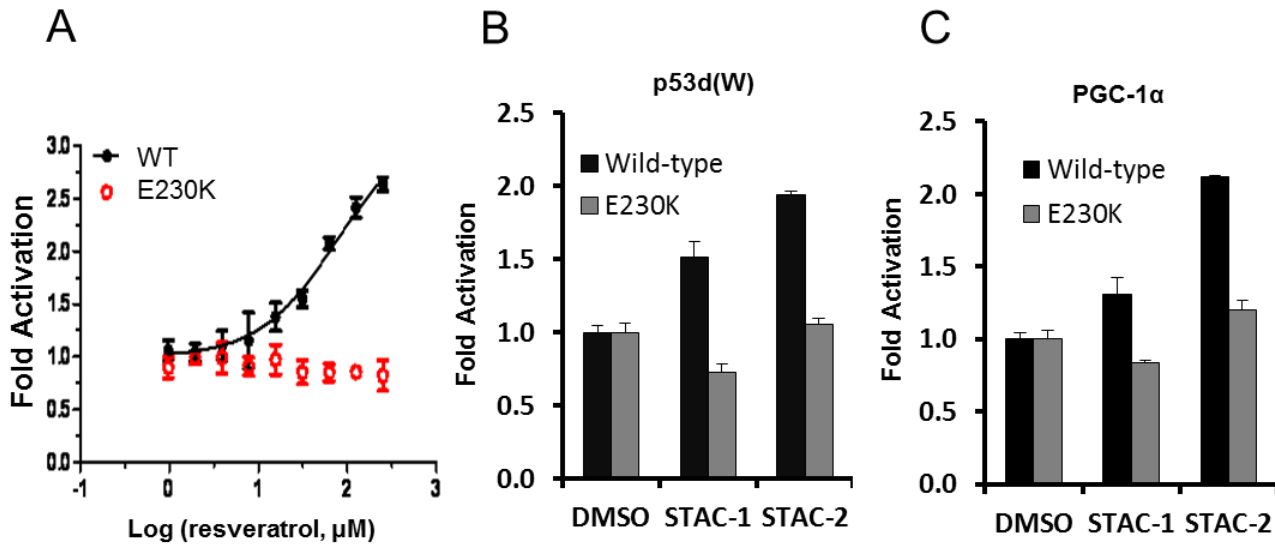


**Fig. S7.** Identification of potential SIRT1 targets which support STAC-mediated activation. **A)** Number of acetylated peptide sequences from nuclear proteins conforming to the indicated consensus sequences, present in the PhosphoSitePlus database (<http://www.phosphosite.org/>). Several examples corresponding to each consensus sequence, and the union of the two sets, are listed. Hydrophobic residues at pertinent positions are indicated in red. **B)** SIRT1 activation by STAC-2 on native sequences predicted to be activated by STACs. **C)** SIRT1 activation by STAC-2 on peptides derived from FOXO3a-242. STAC-2 was used at a dose of 5  $\mu$ M. The PNC1-OPT assay was used to generate the data in panels B and C; mean + SEM (n = 3).



**D**

### Alignment of E230 in SIRT1 homologs in lower organisms

```

Human SIRT1      AIGYRDNLLFGDEIITNGFHSC--SDEEDRASHASSSDWTPRPRIGPYT 186
Monkey SIRT1    AIGYRDNLLFGDEIITNGFHSC--SDEEDRASHASSSDWTPRPRIGPYT 182
Cow SIRT1       AIGYRDNLLFGDEIITNGFHSC--SDEEDRASHASSSDWTPRPRIGPYT 171
Mouse SIRT1     AIGYRDNLLLDGLLTNGFHSC--SDDDR TSHASSSDWTPRPRIGPYT 178
Chicken SIRT1   PAPQPDNFFLLSDEIIANGFHSCD--SDEDDRASHASSSDWTPRPRIGPYT 197
Zebrafish SIRT1 SE-----LTDEGVHPNGFTSPDLLRDDDCCSSRASSDWTFPQPQIGSYR 123
Fly Sir2        -----DDEEGITGTSNED--EDSSNCSSSVDPDWKLR----- 152
Worm Sir2.1     -----ISDAPE TNDSSRQ---RTESTTSVSSSWQNDMMNLR 76
Yeast Sir2      NAR-MFLKYYGAHKFLD TYLPEDLNSLYIYYLIKLLGFVVKDQALIGTIN 185

```

```

Human SIRT1      FVQQHLMIGTDPRTILKDLLPETIP--PPELDDMTLWQIVINILSEPPKR 234
Monkey SIRT1    FVQQHLMIGTDPRTILKDLLPETIP--PPELDDMTLWQIVINILSEPPKR 230
Cow SIRT1       FVQQHLMIGTDPRTILKDLLPETIP--PPELDDMTLWQIVINILSEPPKR 219
Mouse SIRT1     FVQQHLMIGTDPRTILKDLLPETIP--PPELDDMTLWQIVINILSEPPKR 226
Chicken SIRT1   FVQQHLMIGTDPRTILKDLLPETIP--PPELDDMTLWQIVINILSEPPKR 245
Zebrafish SIRT1 FVQQHIMRGTDPRAILKDLLPETV--PPDLDDMTLWQIIINIS-EPKPR 170
Fly Sir2        WLQRFYTGVRVPRQVIASIMPHFATGLAGDTDDSVLWDYLAHLLNEPKRR 202
Worm Sir2.1     RAQRLLDDGATPLQIIQQIFPFDNASRIATMSENAHFAILSDLLERAPVR 126
Yeast Sir2      SIVHINSQERVQDLGSAISVTNVEDPLAKKQTVRLIKDLQRAINKVLCTR 235

```

```

Human SIRT1      KKRKDINTIEDAVKLLQECKKIIVLTGAGVSVSCGIPDFRSRDGIYARLA 284
Monkey SIRT1    KKRKDINTIEDAVKLLQECKKIIVLTGAGVSVSCGIPDFRSRDGIYARLA 280
Cow SIRT1       KKRKDINTIEDAVKLLQECKKIIVLTGAGVSVSCGIPDFRSRDGIYARLA 269
Mouse SIRT1     KKRKDINTIEDAVKLLQECKKIIVLTGAGVSVSCGIPDFRSRDGIYARLA 276
Chicken SIRT1   KKRKDVNTIDDAVKLLQECKKIMVLTGAGVSVSCGIPDFRSRDGIYARLA 295
Zebrafish SIRT1 KKRKDINTLEDVVRLLNERKKILVLTGAGVSVSCGIPDFRSRDGIYARLA 220
Fly Sir2        NKLASVNTFDDVIVSLVKKSSQKIIVLTGAGVSVSCGIPDFRSTNGIYARLA 252
Worm Sir2.1     QKLTNYSNLADAVELFKTKKHILVLTGAGVSVSCGIPDFRSKDIYARLR 176
Yeast Sir2      LRLSNFFTIDHFIQKLTARKILVLTGAGVSTSLGIPDFRSSEGFYS--K 283

```

**Fig. S8.** Effect of E230 on natural peptide activation by resveratrol and sequence conservation. **A)** Dose response titrations of resveratrol on wild-type SIRT1 and SIRT1-E230K activity using the Trp 5-mer peptide, using the OAcADPR assay; mean  $\pm$  SD (n = 3). **B)** Activation of wild-type and SIRT1-E230K by two STACs using the p53d(W) substrate. **C)** Activation of wild-type and SIRT1-E230K by two STACs using the PGC-1 $\alpha$ -778 substrate. **D)** ClustalW sequence alignment of E230 (yellow) in human SIRT1 with SIRT1/Sir2 homologs in several organisms. STAC-1 and STAC-2 were used at concentrations of 50  $\mu$ M and 5  $\mu$ M, respectively. Data for panels B and C were generated using the PNC1-OPT assay; mean + SEM (n = 3).

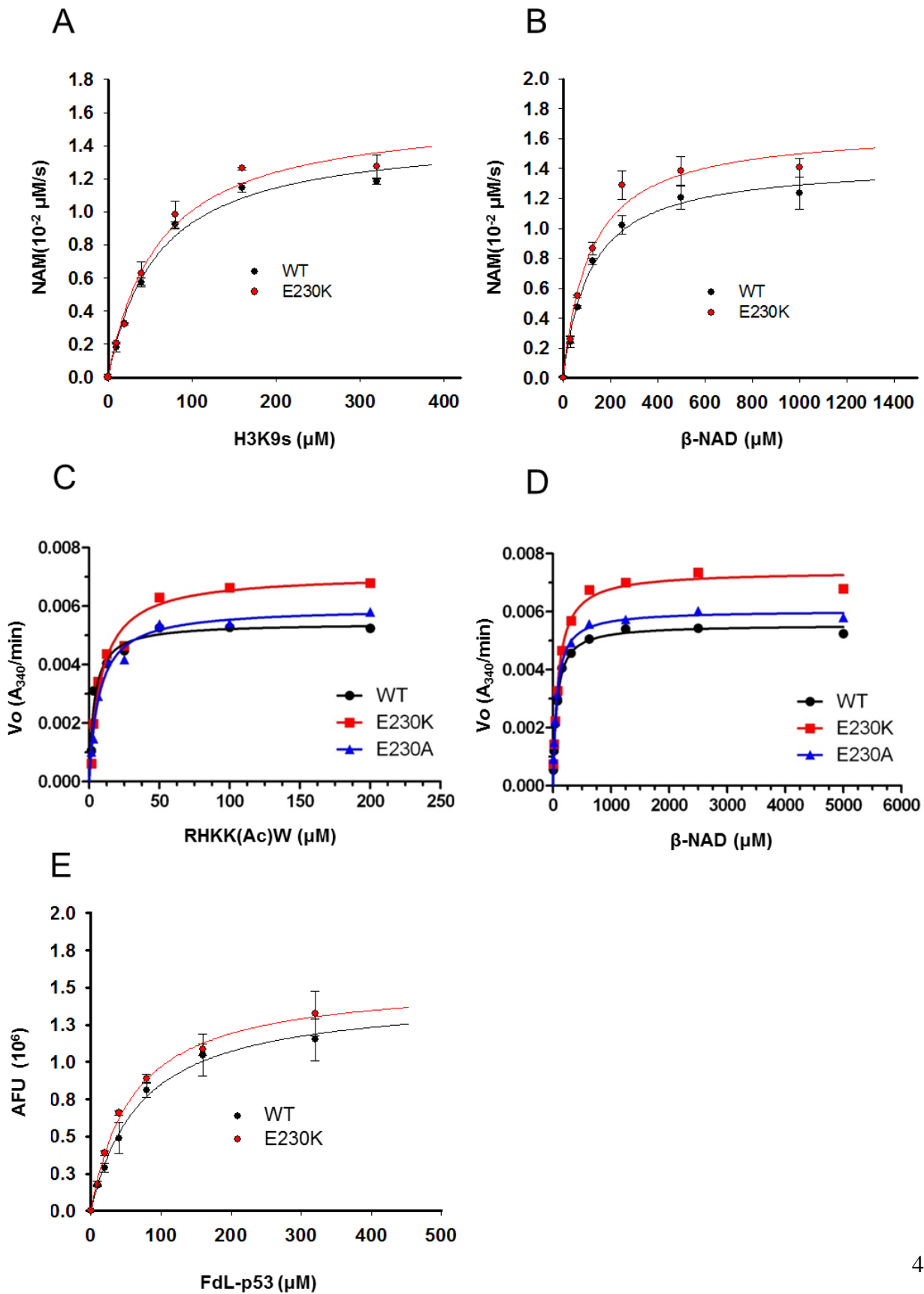
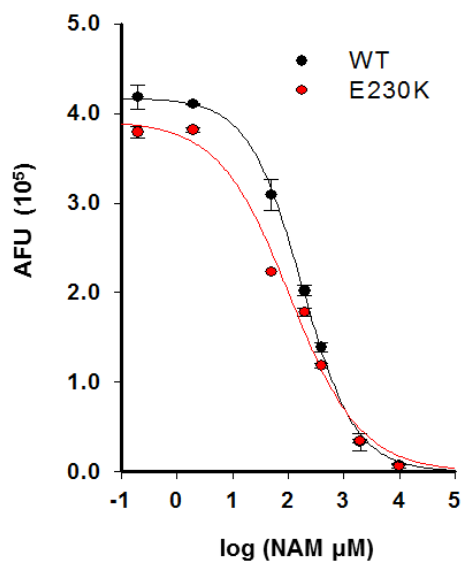
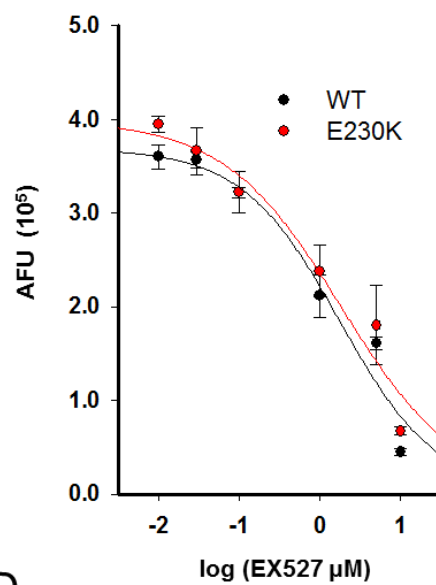


**Fig. S9.** Comparison of wild-type SIRT1 and SIRT1-E230K kinetics. Comparison of **A)**  $K_{M\text{H3K9}}$  peptide, or **B)**  $K_{M\text{B-NAD}^+}$  between wild-type SIRT1 and SIRT1-E230K using the PNC1-OPT assay; mean  $\pm$  SEM shown ( $n = 3$ ). Comparison of **C)**  $K_{M\text{Trp 5-mer}}$  peptide, or **D)**  $K_{M\text{B-NAD}^+}$  between wild-type SIRT1 SIRT1-E230K, and SIRT1-E230A using the PNC1/GDH assay. **E)** Comparison of  $K_{M\text{FdL-p53}}$  between wild-type SIRT1 and SIRT1-E230K using the BIOMOL assay; mean  $\pm$  SD shown ( $n = 3$ ).

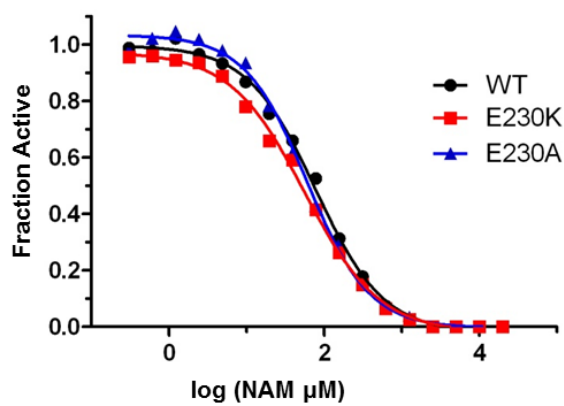
A



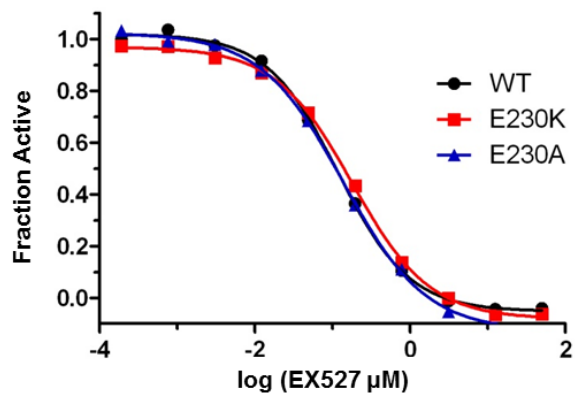
B



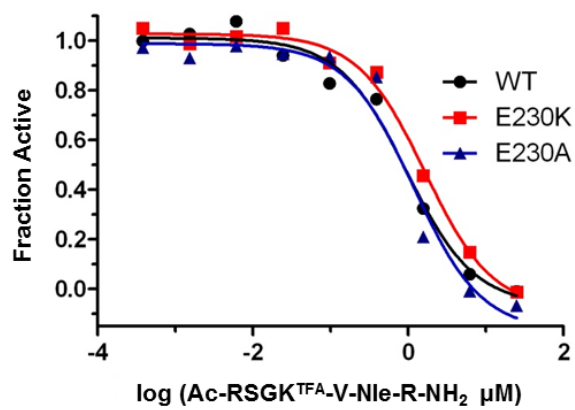
C



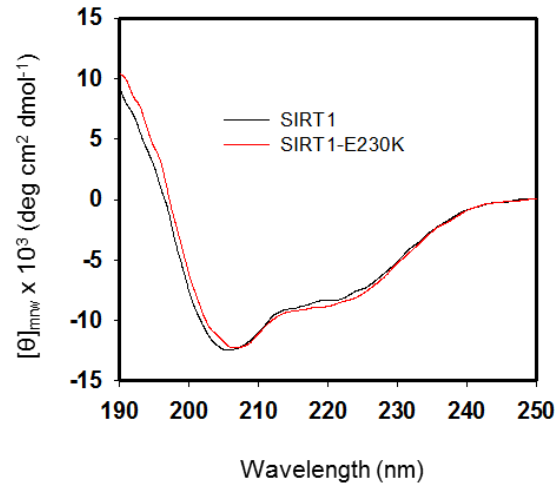
D



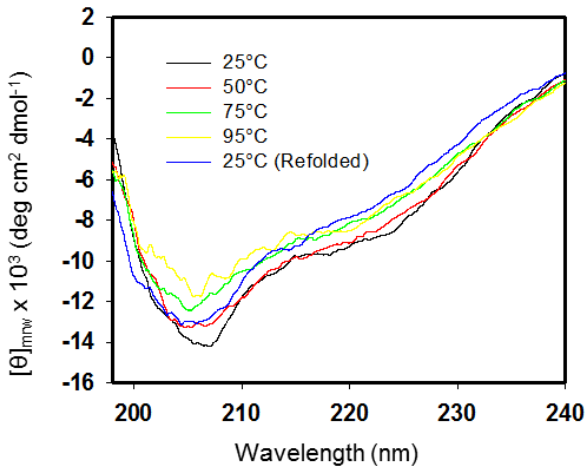
E



**Fig. S10.** Inhibition profiles for wild-type SIRT1 and SIRT1-E230. Comparison of wild-type SIRT1 and SIRT-E230K inhibition by **A)** NAM or **B)** EX-527 using the BIOMOL assay; mean  $\pm$  SD shown (n = 2). Comparison of SIRT1, SIRT1-E230K, and SIRT1-E230A inhibition by **C)** nicotinamide, or **D)** EX-527, or **E)** TFA ACS2 peptide using the OAcADPR assay.

**A****B**

Thermal Denaturation:  
SIRT1(Wild-type)

**C**

Thermal Denaturation:  
SIRT1(E230K)

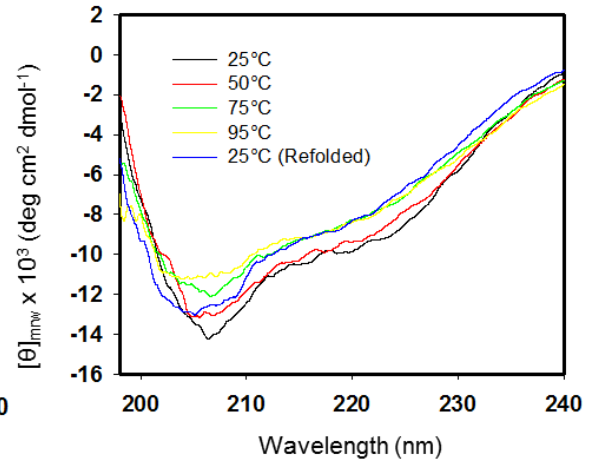
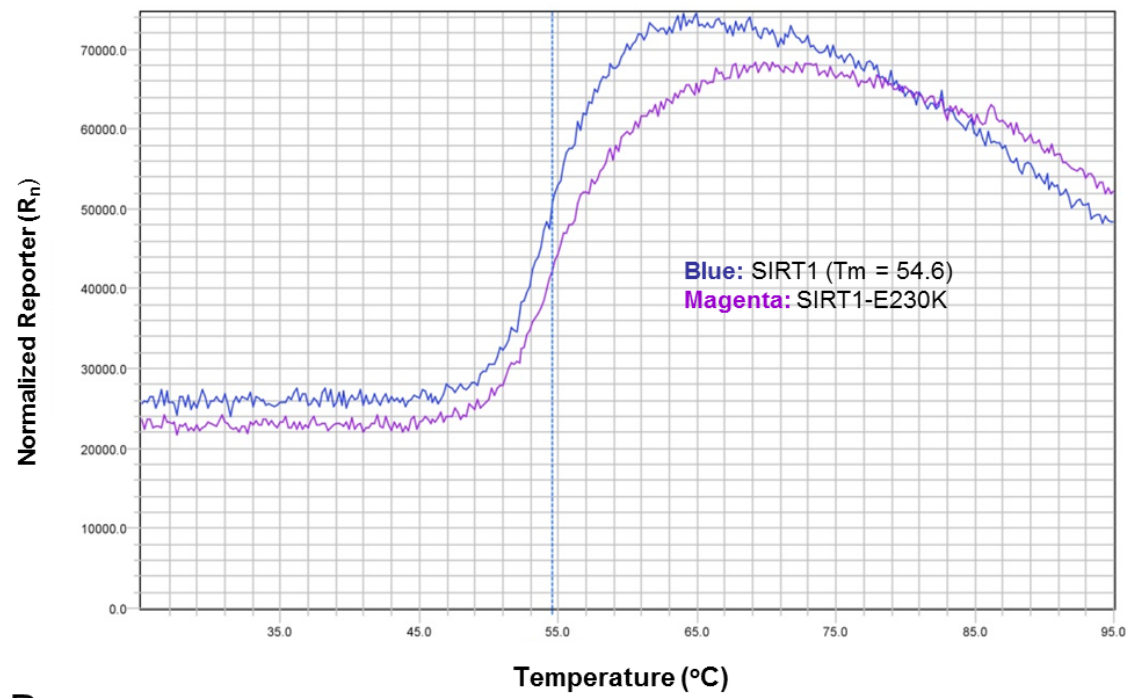


**Fig. S11.** Circular dichroism (CD) analysis of wild-type and SIRT1-E230K structure. **A)** CD spectra of SIRT1 and SIRT1-E230K proteins in the absence of ligand at ambient temperature. Thermal melting spectra of **B)** wild-type SIRT1, or **C)** SIRT1-E230K at the indicated temperatures.

A



B

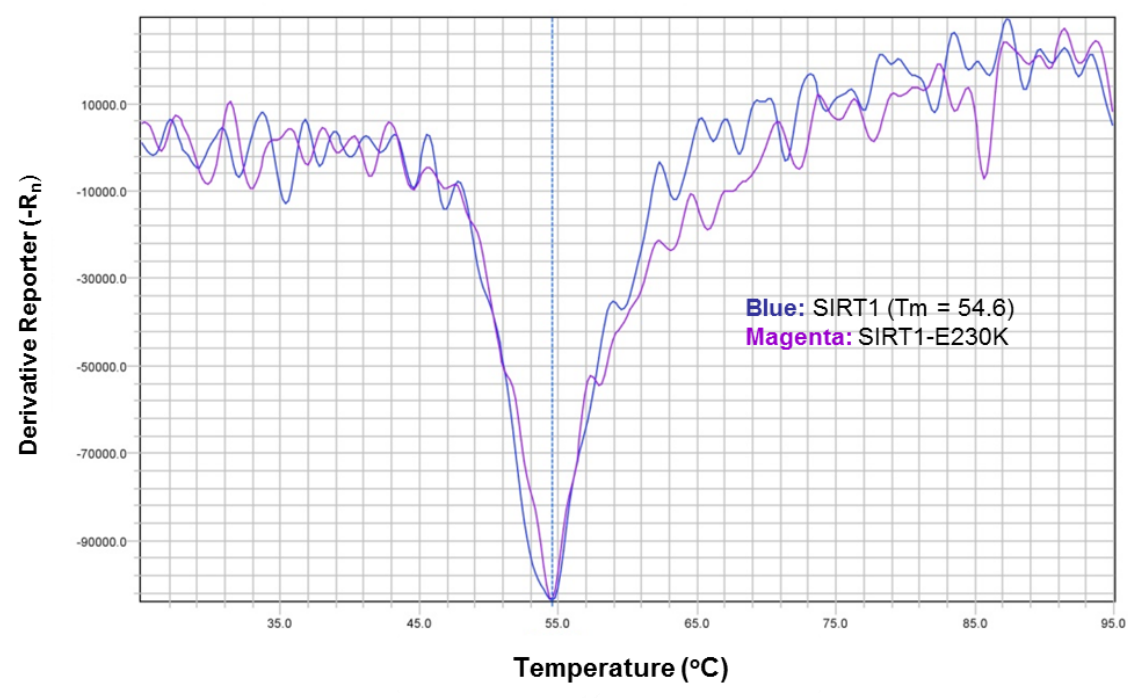


**Fig. S12.** Thermal shift analysis of wild-type SIRT1 and SIRT-E230K melting temperatures. Wild-type SIRT1 and SIRT1-E230K spectra showing **A)** normalized reporter values, and **B)** derivative reporter values. The calculated melting temperature of wild-type SIRT1 is indicated.

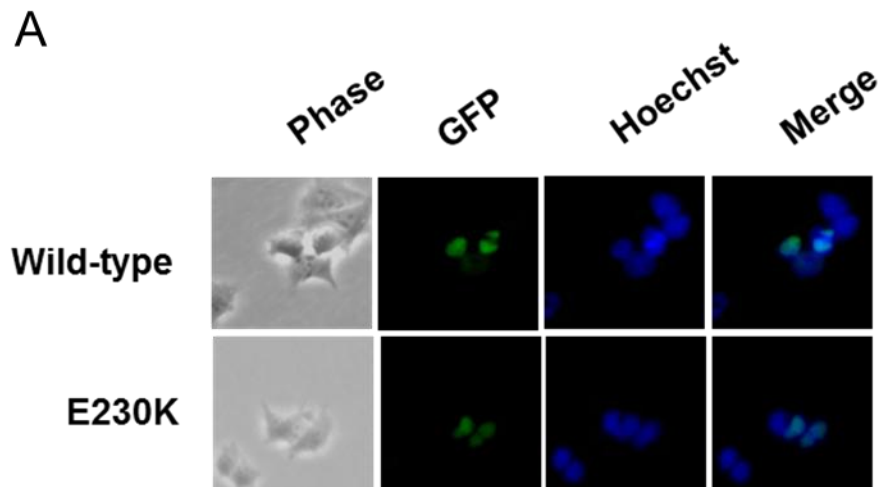


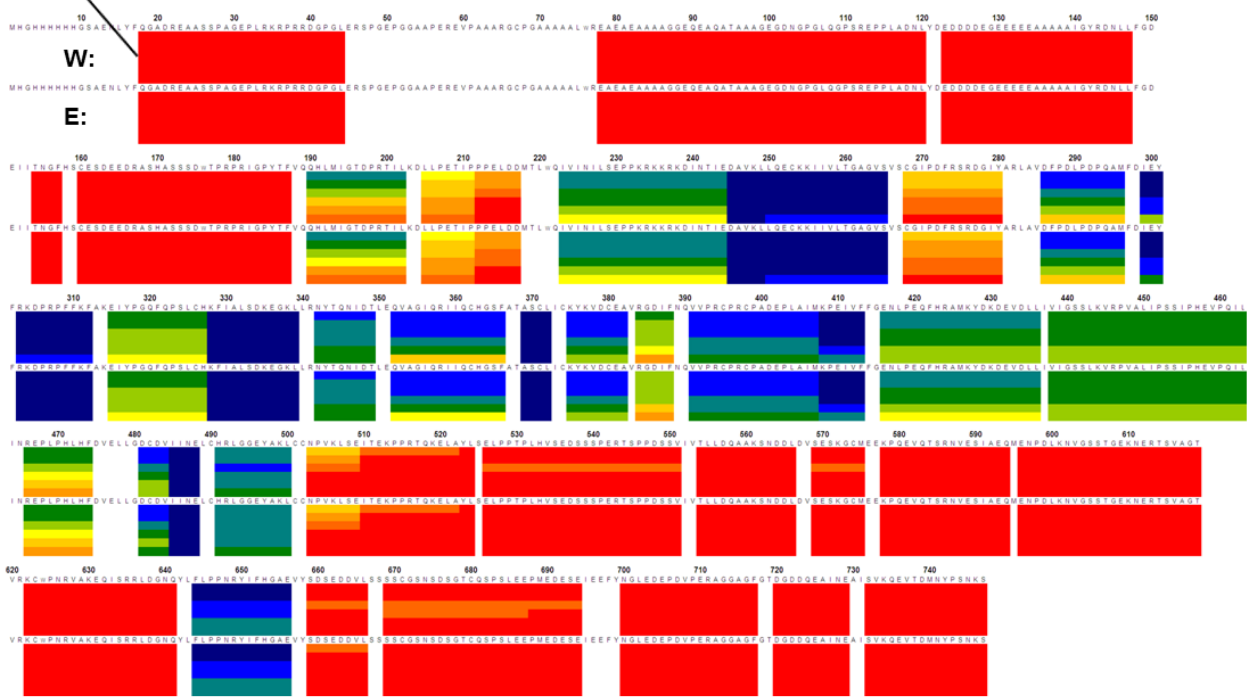
**Fig. S13.** SIRT1-E230K localization. A) Localization of wild-type SIRT1 and SIRT1-E230K GFP-fusions in transiently transfected 293-T cells co-stained with Hoechst fluorescent DNA dye.

A

Deuteration Level

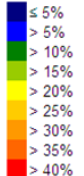


- 1: 15 s
- 2: 50 s
- 3: 150 s
- 4: 500 s
- 5: 1500 s
- 6: 5000 s

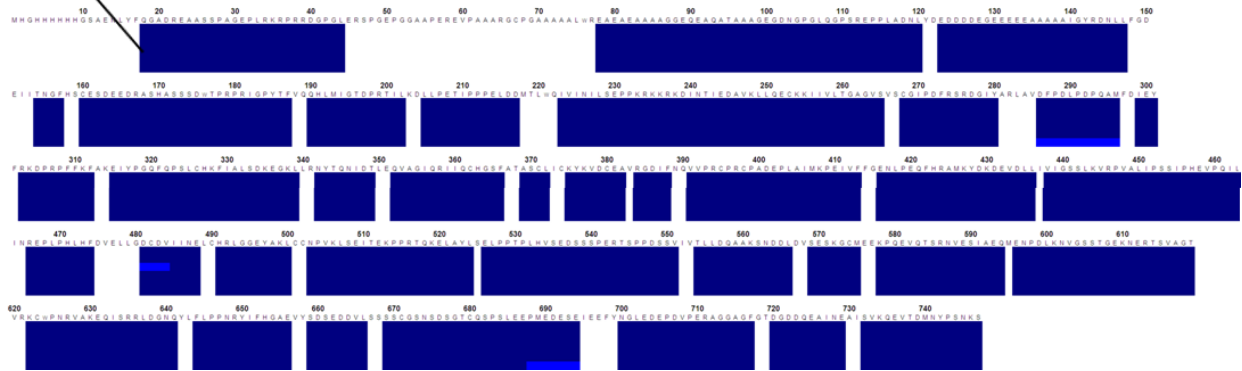


B

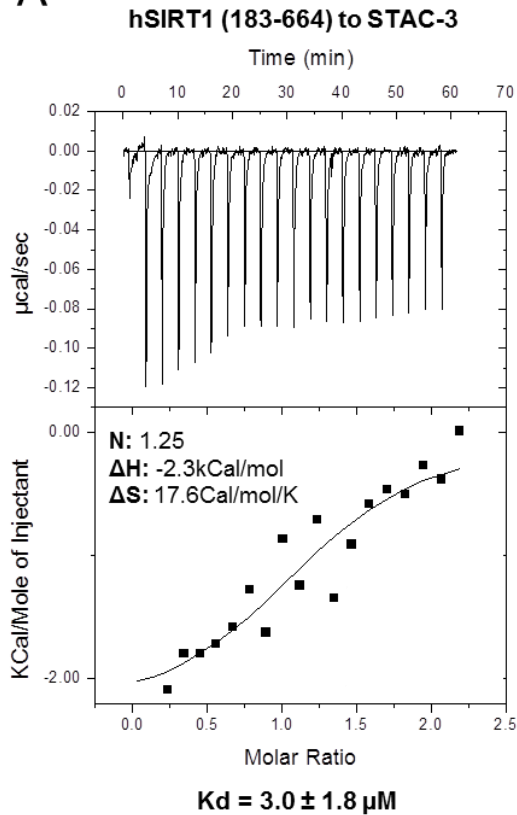
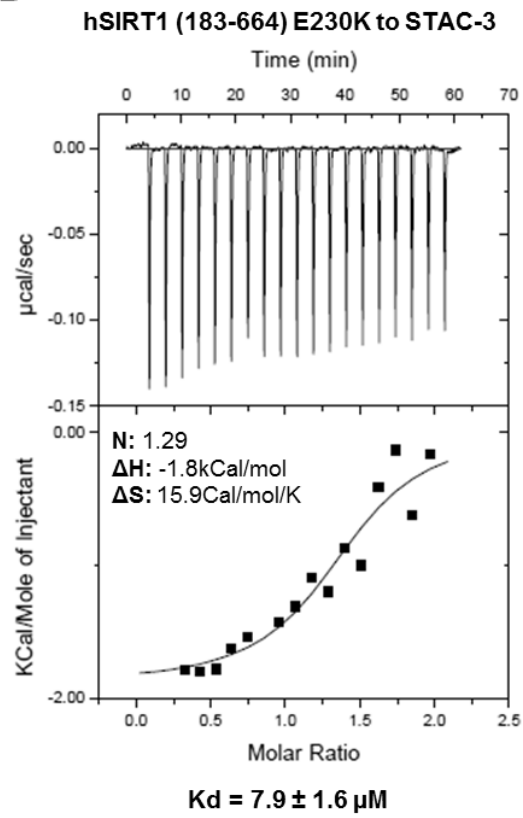
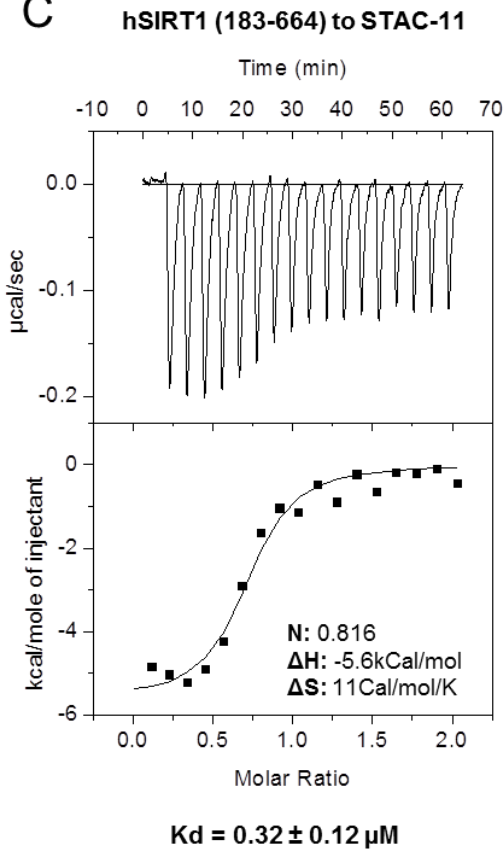
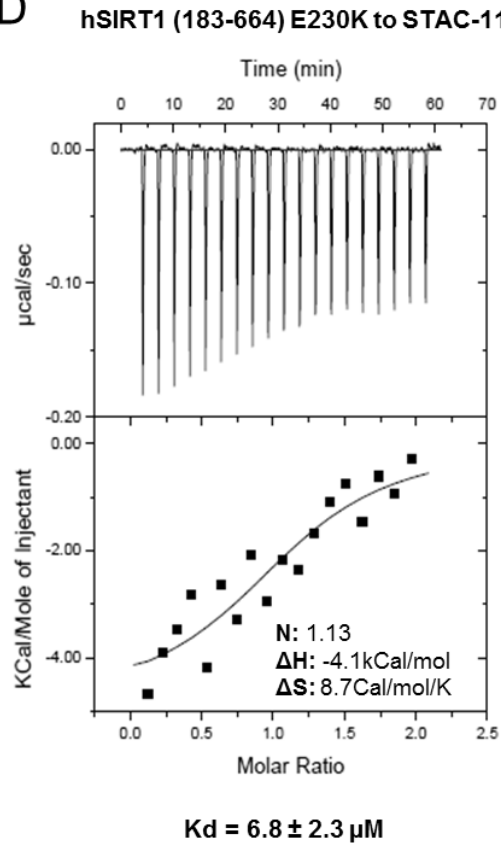
Perturbation



- 1: 15 s
- 2: 50 s
- 3: 150 s
- 4: 500 s
- 5: 1500 s
- 6: 5000 s

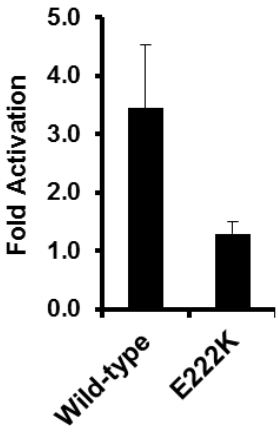


**Fig. S14.** Hydrogen-deuterium exchange mass spectrometry (HDXMS) analysis of wild-type SIRT1 and SIRT1-E230K protein dynamics. **A)** Heat-map illustrating deuteration levels of wild-type (W) and SIRT1-E230K (E) at six different time points (shown in black). **B)** Heat-map illustrating the relative perturbation differences between wild-type SIRT1 and SIRT1-E230K at six different time points (shown in black).

**A****B****C****D**

**Fig. S15.** Binding of STACs to wild-type SIRT1 and SIRT1-E230K determined using isothermal titration calorimetry. Binding of STAC-3 or STAC-11 to wild-type SIRT1 (**A**, **C**), and SIRT1-E230K (**B**, **D**), respectively. Stoichiometry, and enthalpy/entropy changes are included in the panel insets.  $K_d$  values  $\pm$  curve-fit errors are indicated underneath each plot.

**A**



**B**

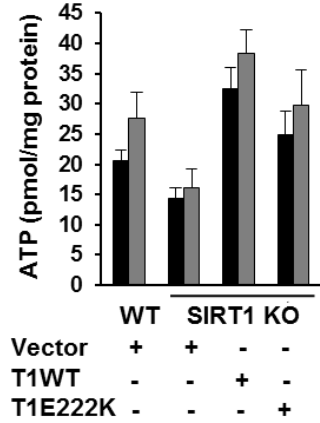
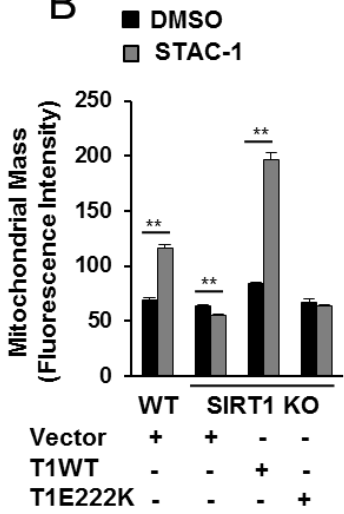
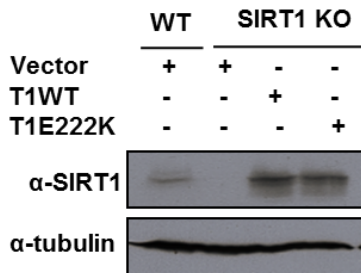
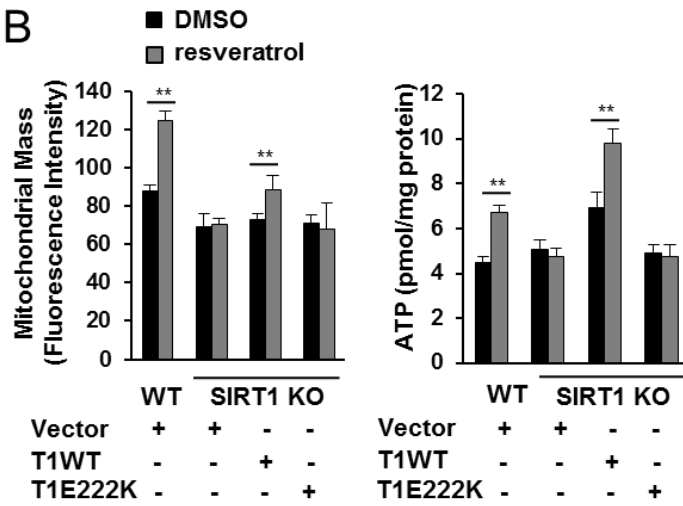


**Fig. S16.** SIRT1-E222K activation and its effects on STAC-mediated mitochondrial-related parameters in primary myoblasts. **A)** Fold-activation of wild-type SIRT1 and SIRT1-E222K in the presence or absence of resveratrol, measured using the BIOMOL assay; mean + s.d (n=4). **B)** Effect of SIRT1-E222K substitution on mitochondrial mass and ATP content in primary myoblasts following 24 hr treatment with 1  $\mu$ M STAC-1; mean + s.e. (n=6). \*\* indicates  $P < 0.01$  (t-test) with respect to the DMSO control.

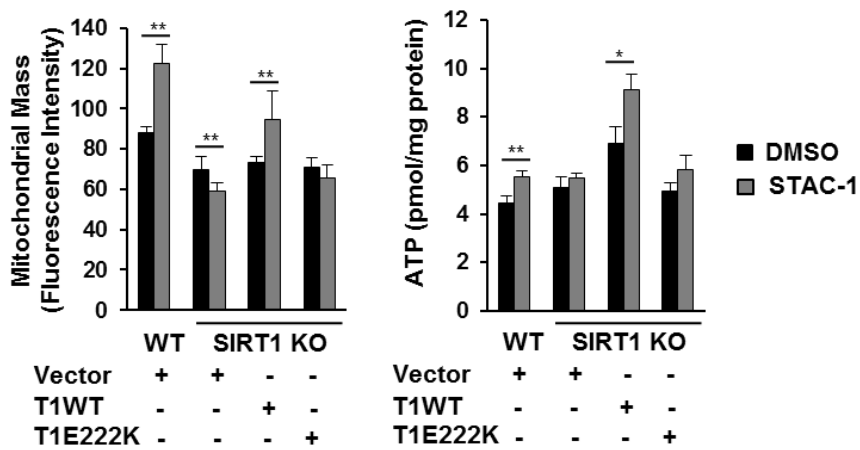
**A**



**B**



**C**



**D**

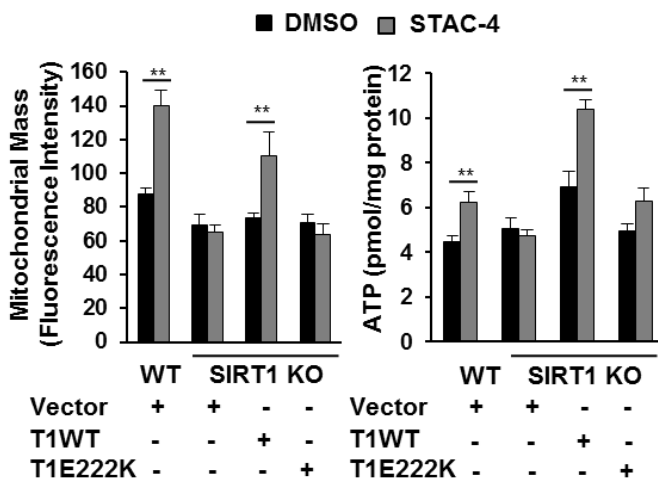


**Fig. S17.** Effects of E222K on STAC-mediated mitochondrial-related parameters in MEFs. **A)** SIRT1 protein expression levels in wild-type mouse embryonic fibroblasts (MEFs), or SIRT1 KO MEFs reconstituted with empty adenovirus, or adenovirus carrying wild-type mSIRT1 or mSIRT1-E222K. Effect of **B)** resveratrol, **C)** STAC-1, and **D)** STAC-4 on mitochondrial mass and ATP content in MEFs reconstituted with either wild-type mSIRT1 or mSIRT1-E222K following 24 hr treatment; mean + s.e. shown (n=6). Resveratrol, STAC-1, and STAC-4 were used at doses of 25  $\mu$ M, 1  $\mu$ M, and 1  $\mu$ M, respectively. \* indicates  $P < 0.05$  (t-test), \*\* indicates  $P < 0.01$  (t-test) with respect to the DMSO control.

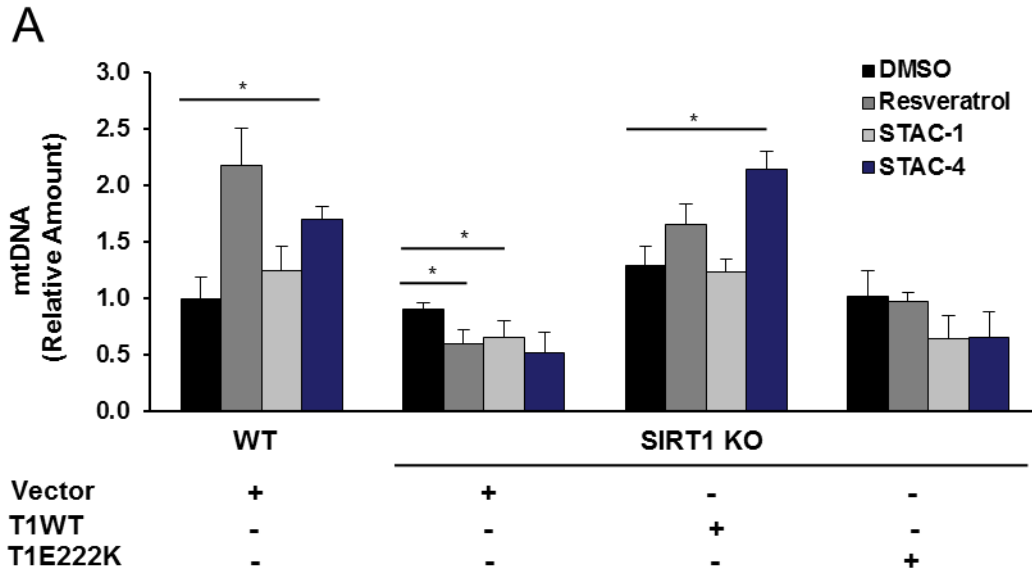


**Fig. S18.** Effect of E222K on STAC-mediated induction of mtDNA in MEFs.

A) Effect of SIRT1-E222K substitution on STAC-mediated mitochondrial DNA induction in MEFs (24 hr treatment); mean + s.e. (n=5). Resveratrol, STAC-1 and STAC-4 were used at 25  $\mu$ M, 1  $\mu$ M, and 1  $\mu$ M, respectively. \* indicates  $P < 0.05$  (t-test) with respect to DMSO control.

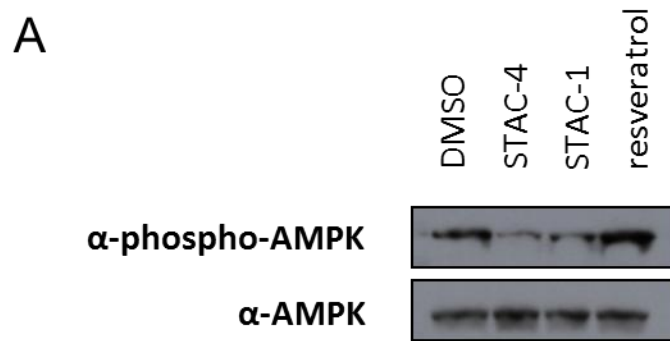
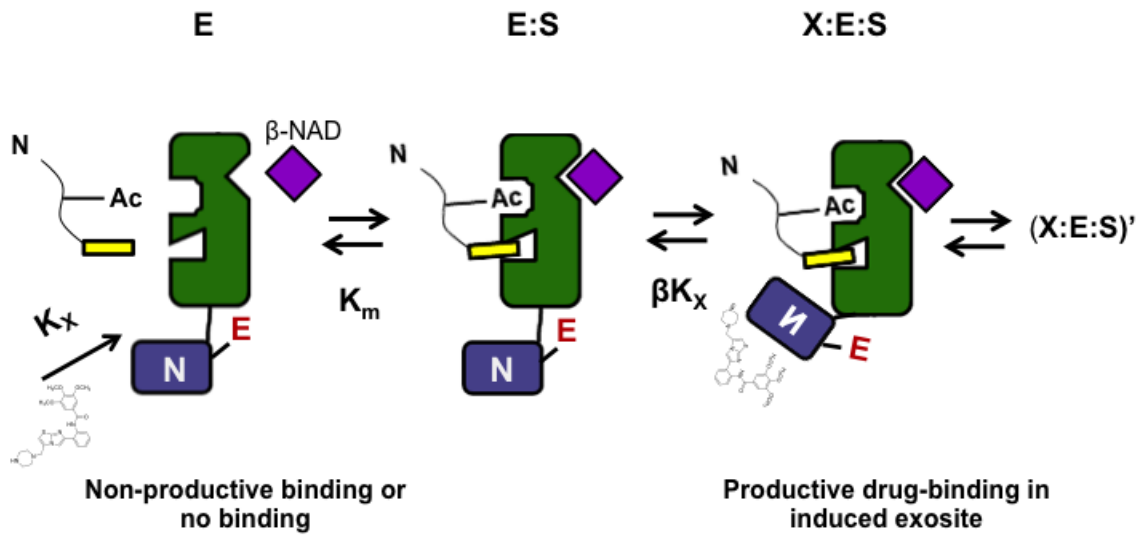


**Fig. S19.** AMPK activation by STACs. **A)** AMP-activated kinase (AMPK) phosphorylation levels in MEFs following 24 hrs of STAC treatment. Resveratrol, STAC-1 and STAC-4 were used at doses of 25  $\mu$ M, 1  $\mu$ M, and 1  $\mu$ M, respectively, and cell extracts were probed for phosphorylated (activated) and total AMPK by western blotting.

### A Substrate-assisted allosteric activation

 Hydrophobic residues



### B Factor-assisted allosteric activation

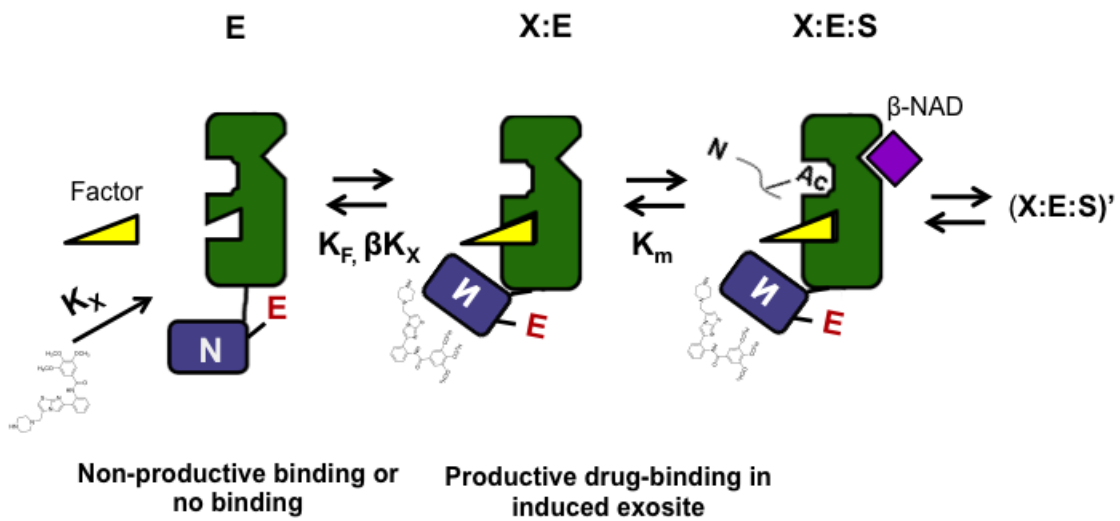


**Fig. S20.** Models of assisted allosteric activation (AAA) of SIRT1 by small molecules. Diagrams outlining **A)** substrate-assisted allosteric activation and **B)** factor-assisted allosteric activation. Yellow box indicates hydrophobic residues C-terminal to the acetylated lysine. The inverted N indicates the conformation of the N-terminus that supports the activated state when STACs are bound to the activation domain, which may be facilitated by interactions with the C-terminus and/or catalytic domain. The red “E” represents E230, whose negative charge may interact with a positively-charged amino acid in SIRT1 to facilitate allosteric activation. E=enzyme; S=substrate; X=STAC; X:E:S=activator:enzyme:substrate complex;  $K_X$ =activator equilibrium constant;  $K_M$ =Michaelis constant;  $\beta K_X$ =activator equilibrium constant in the presence of a docked substrate/factor;  $K_F$ =factor equilibrium constant.

**Table S1.** EC<sub>50</sub> values for STACs derived from Fig. S4A.

	<b>EC<sub>50</sub> (μM)</b>
STAC-1	21.9 ± 1.1
STAC-2	1.0 ± 1.1
STAC-4	8.8 ± 1.3
resveratrol	29.5 ± 1.1

± curve-fit errors

**Table S2.** Kinetic parameters corresponding to titrations in Fig. S4, B and C.

	<b>FdL-p53 titration</b>		<b><math>\beta</math>-NAD<sup>+</sup> titration</b>	
	<b>V<sub>max</sub> (AFU x 10<sup>5</sup>)</b>	<b>K<sub>M</sub> (<math>\mu</math>M)</b>	<b>V<sub>max</sub> (AFU x 10<sup>5</sup>)</b>	<b>K<sub>M</sub> (<math>\mu</math>M)</b>
DMSO	2.62 $\pm$ 0.09	130.9 $\pm$ 10.6	2.01 $\pm$ 0.05	451.0 $\pm$ 40.7
STAC-1	2.50 $\pm$ 0.11	25.0 $\pm$ 4.8	1.74 $\pm$ 0.02	223.7 $\pm$ 12.2
STAC-2	2.50 $\pm$ 0.11	23.9 $\pm$ 4.6	2.47 $\pm$ 0.05	221.4 $\pm$ 16.7
STAC-4	2.25 $\pm$ 0.09	36.8 $\pm$ 5.5	2.22 $\pm$ 0.09	298.8 $\pm$ 47.4
resveratrol	2.47 $\pm$ 0.10	5.0 $\pm$ 2.6	2.48 $\pm$ 0.04	98.0 $\pm$ 6.6

$\pm$  curve-fit errors

**Table S3.** Activation parameters corresponding to titrations in Fig. 3, A and B.

Compound	WT		E230K		E230A	
	EC <sub>1.5</sub> ( $\mu$ M)	Max. Activation <sup>a</sup>	EC <sub>1.5</sub> ( $\mu$ M)	Max. Activation <sup>a</sup>	EC <sub>1.5</sub> ( $\mu$ M)	Max. Activation <sup>a</sup>
STAC-5	0.40	13.1	19	1.7	3.6	3.2
STAC-8	1.2	8.9	>50	1.4	17	2.2

<sup>a</sup> = maximum observed fold-activation

**Table S4.** Fold activation of SIRT1-WT and SIRT1-E230K using newly described STACs on three distinct substrates, using three different assays.

	BIOMOL Assay (FdL-p53 substrate)		PNC1-OPT Assay (p53d(W) substrate)		OAcADPR Assay (RHKK(Ac)W substrate)	
	WT	E230K	WT	E230K	WT	E230K
<b>STAC-5</b>	1.79 ± 0.15	1.29 ± 0.07	1.66 ± 0.19	1.29 ± 0.12	6.17	1.14
<b>STAC-6</b>	2.73 ± 0.09	1.96 ± 0.09	1.49 ± 0.07	0.95 ± 0.12	4.66	1.72
<b>STAC-7</b>	2.06 ± 0.03	1.36 ± 0.15	1.45 ± 0.15	1.05 ± 0.09	2.57	1.36
<b>STAC-9</b>	1.92 ± 0.02	0.71 ± 0.11	1.50 ± 0.03	1.01 ± 0.09	5.71	1.67
<b>STAC-10</b>	3.60 ± 0.27	1.87 ± 0.09	1.43 ± 0.03	0.98 ± 0.09	3.83	1.37

Mean ± S.D. (n=3) is shown for BIOMOL and OAcADPR, ± S.E. for PNC1-OPT assay (n=3).

**Table S5.** Comparison of WT, E230K, and E230A SIRT1 IC<sub>50</sub>s corresponding to titrations in Fig. S10, C to E.

Inhibitor	WT	IC <sub>50</sub> (μM)	
		E230K	E230A
TFA ACS2 peptide	1.0 ± 0.2	1.7 ± 0.3	1.2 ± 0.4
Nicotinamide	78 ± 5	57 ± 4	60 ± 4
EX-527	0.12 ± 0.01	0.18 ± 0.01	0.13 ± 0.01

± curve-fit errors

**Table S6.** Deconvolution of SIRT1-WT and SIRT1-E230K CD Spectra.

	<b><math>\alpha</math>- helix(r*)</b>	<b><math>\alpha</math>- helix(d*)</b>	<b><math>\beta</math>- sheet(r*)</b>	<b><math>\beta</math>- sheet(d*)</b>	<b>Turn</b>	<b>Unord.</b>
<b>SIRT1-WT</b>						
CONTINLL	0.121	0.130	0.117	0.083	0.221	0.327
SELCON3	0.120	0.125	0.125	0.083	0.222	0.319
CDSSTR	0.115	0.121	0.127	0.089	0.219	0.325
<b>SIRT1-E230K</b>						
CONTINLL	0.133	0.133	0.109	0.082	0.220	0.324
SELCON3	0.132	0.129	0.117	0.082	0.222	0.318
CDSSTR	0.126	0.124	0.132	0.091	0.216	0.209

\*r=regular, d=distorted

**Table S7.** Comparison of STAC-3 binding and enzyme activation for several SIRT1 truncations and SIRT1-E230K.

Construct	Fold Activation (FdL-p53)	K <sub>d</sub> (μM) ITC
SIRT1(183-664)	1.8 ± 0.01	3.0 ± 1.8
SIRT1(183-664)-E230K	1.1 ± 0.1	7.9 ± 1.6
SIRT1(195-664)	1.2 ± 0.2	Not detectable
SIRT1(225-664)	1.1 ± 0.1	Not detectable

Basal enzyme kinetic parameters for all four constructs were comparable. Mean ± S.D. (n=3) is shown for activation, ± curve-fit errors for binding.

**Table S8.** Effects of STACs on the activity of major PDE isoforms.

STAC (Dose)	PDE3B		PDE4B1	
	% Inhib. 1	% Inhib. 2	% Inhib. 1	% Inhib. 2
STAC-1 (1 $\mu$ M)	3.68	1.69	0.72	-5.53
STAC-4 (1 $\mu$ M)	8.29	5.83	-6.17	1.70
Resveratrol (10 $\mu$ M)	19.74	14.68	1.14	4.73
Resveratrol (25 $\mu$ M)	11.61	6.60	9.24	13.93

Two reference compounds were assayed alongside the above samples as positive controls.

## References and Notes

1. C. Sebastian, K. F. Satterstrom, M. C. Haigis, R. Mostoslavsky, From sirtuin biology to human diseases: An update. *J. Biol. Chem.* **287**, 42444 (2012).  
[doi:10.1074/jbc.R112.402768](https://doi.org/10.1074/jbc.R112.402768)
2. M. C. Haigis, D. A. Sinclair, Mammalian sirtuins: Biological insights and disease relevance. *Annu. Rev. Pathol.* **5**, 253 (2010). [doi:10.1146/annurev.pathol.4.110807.092250](https://doi.org/10.1146/annurev.pathol.4.110807.092250) [Medline](#)
3. A. Chalkiadaki, L. Guarente, Sirtuins mediate mammalian metabolic responses to nutrient availability. *Nat. Rev. Endocrinol.* **8**, 287 (2012). [Medline](#)
4. K. T. Howitz *et al.*, Small molecule activators of sirtuins extend *Saccharomyces cerevisiae* lifespan. *Nature* **425**, 191 (2003). [doi:10.1038/nature01960](https://doi.org/10.1038/nature01960) [Medline](#)
5. J. C. Milne *et al.*, Small molecule activators of SIRT1 as therapeutics for the treatment of type 2 diabetes. *Nature* **450**, 712 (2007). [doi:10.1038/nature06261](https://doi.org/10.1038/nature06261) [Medline](#)
6. J. A. Baur *et al.*, Resveratrol improves health and survival of mice on a high-calorie diet. *Nature* **444**, 337 (2006). [doi:10.1038/nature05354](https://doi.org/10.1038/nature05354) [Medline](#)
7. R. K. Minor *et al.*, SRT1720 improves survival and healthspan of obese mice. *Sci. Rep.* **1**, 70 (2011). [doi:10.1038/srep00070](https://doi.org/10.1038/srep00070)
8. M. Kaeberlein *et al.*, Substrate-specific activation of sirtuins by resveratrol. *J. Biol. Chem.* **280**, 17038 (2005). [doi:10.1074/jbc.M500655200](https://doi.org/10.1074/jbc.M500655200) [Medline](#)
9. M. T. Borra, B. C. Smith, J. M. Denu, Mechanism of human SIRT1 activation by resveratrol. *J. Biol. Chem.* **280**, 17187 (2005). [doi:10.1074/jbc.M501250200](https://doi.org/10.1074/jbc.M501250200) [Medline](#)
10. M. Pacholec *et al.*, SRT1720, SRT2183, SRT1460, and resveratrol are not direct activators of SIRT1. *J. Biol. Chem.* **285**, 8340 (2010). [doi:10.1074/jbc.M109.088682](https://doi.org/10.1074/jbc.M109.088682) [Medline](#)
11. D. Beher *et al.*, Resveratrol is not a direct activator of SIRT1 enzyme activity. *Chem. Biol. Drug Des.* **74**, 619 (2009). [doi:10.1111/j.1747-0285.2009.00901.x](https://doi.org/10.1111/j.1747-0285.2009.00901.x) [Medline](#)
12. M. Ghislain, E. Talla, J. M. François, Identification and functional analysis of the *Saccharomyces cerevisiae* nicotinamidase gene, PNC1. *Yeast* **19**, 215 (2002).  
[doi:10.1002/yea.810](https://doi.org/10.1002/yea.810) [Medline](#)

13. K. Sugawara, F. Oyama, Fluorogenic reaction and specific microdetermination of ammonia. *J. Biochem.* **89**, 771 (1981). [Medline](#)
14. A. A. Sauve, C. Wolberger, V. L. Schramm, J. D. Boeke, The biochemistry of sirtuins. *Annu. Rev. Biochem.* **75**, 435 (2006). [doi:10.1146/annurev.biochem.74.082803.133500](https://doi.org/10.1146/annurev.biochem.74.082803.133500) [Medline](#)
15. H. Dai *et al.*, SIRT1 activation by small molecules: Kinetic and biophysical evidence for direct interaction of enzyme and activator. *J. Biol. Chem.* **285**, 32695 (2010). [doi:10.1074/jbc.M110.133892](https://doi.org/10.1074/jbc.M110.133892) [Medline](#)
16. Single-letter abbreviations for amino acid residues: A, Ala; C, Cys; D, Asp; E, Glu; F, Phe; G, Gly; H, His; I, Ile; K, Lys; L, Leu; M, Met; N, Asn; P, Pro; Q, Gln; R, Arg; S, Ser; T, Thr; V, Val; W, Trp; Y, Tyr; X, any amino acid.
17. A. Vaquero *et al.*, Human SirT1 interacts with histone H1 and promotes formation of facultative heterochromatin. *Mol. Cell* **16**, 93 (2004). [doi:10.1016/j.molcel.2004.08.031](https://doi.org/10.1016/j.molcel.2004.08.031) [Medline](#)
18. R. Firestein *et al.*, The SIRT1 deacetylase suppresses intestinal tumorigenesis and colon cancer growth. *PLoS ONE* **3**, e2020 (2008). [doi:10.1371/journal.pone.0002020](https://doi.org/10.1371/journal.pone.0002020) [Medline](#)
19. A. Brunet *et al.*, Stress-dependent regulation of FOXO transcription factors by the SIRT1 deacetylase. *Science* **303**, 2011 (2004). [doi:10.1126/science.1094637](https://doi.org/10.1126/science.1094637) [Medline](#)
20. S. Kume *et al.*, SIRT1 inhibits transforming growth factor beta-induced apoptosis in glomerular mesangial cells via Smad7 deacetylation. *J. Biol. Chem.* **282**, 151 (2007). [doi:10.1074/jbc.M605904200](https://doi.org/10.1074/jbc.M605904200) [Medline](#)
21. F. Lan, J. M. Cacicedo, N. Ruderman, Y. Ido, SIRT1 modulation of the acetylation status, cytosolic localization, and activity of LKB1. Possible role in AMP-activated protein kinase activation. *J. Biol. Chem.* **283**, 27628 (2008). [doi:10.1074/jbc.M805711200](https://doi.org/10.1074/jbc.M805711200) [Medline](#)
22. J. T. Rodgers *et al.*, Nutrient control of glucose homeostasis through a complex of PGC-1 $\alpha$  and SIRT1. *Nature* **434**, 113 (2005). [doi:10.1038/nature03354](https://doi.org/10.1038/nature03354) [Medline](#)
23. F. Yeung *et al.*, Modulation of NF- $\kappa$ B-dependent transcription and cell survival by the SIRT1 deacetylase. *EMBO J.* **23**, 2369 (2004). [doi:10.1038/sj.emboj.7600244](https://doi.org/10.1038/sj.emboj.7600244) [Medline](#)

24. C. Das, M. S. Lucia, K. C. Hansen, J. K. Tyler, CBP/p300-mediated acetylation of histone H3 on lysine 56. *Nature* **459**, 113 (2009). [doi:10.1038/nature07861](https://doi.org/10.1038/nature07861) [Medline](#)
25. H. S. Ghosh, B. Reizis, P. D. Robbins, SIRT1 associates with eIF2- $\alpha$  and regulates the cellular stress response. *Sci. Rep.* **1**, 150 (2011). [doi:10.1038/srep00150](https://doi.org/10.1038/srep00150)
26. H. Kang *et al.*, Peptide switch is essential for Sirt1 deacetylase activity. *Mol. Cell* **44**, 203 (2011). [doi:10.1016/j.molcel.2011.07.038](https://doi.org/10.1016/j.molcel.2011.07.038) [Medline](#)
27. M. Pan, H. Yuan, M. Brent, E. C. Ding, R. Marmorstein, SIRT1 contains N- and C-terminal regions that potentiate deacetylase activity. *J. Biol. Chem.* **287**, 2468 (2012). [doi:10.1074/jbc.M111.285031](https://doi.org/10.1074/jbc.M111.285031) [Medline](#)
28. Z. Gerhart-Hines *et al.*, Metabolic control of muscle mitochondrial function and fatty acid oxidation through SIRT1/PGC-1 $\alpha$ . *EMBO J.* **26**, 1913 (2007). [doi:10.1038/sj.emboj.7601633](https://doi.org/10.1038/sj.emboj.7601633) [Medline](#)
29. M. Bernier *et al.*, Negative regulation of STAT3 protein-mediated cellular respiration by SIRT1 protein. *J. Biol. Chem.* **286**, 19270 (2011). [doi:10.1074/jbc.M110.200311](https://doi.org/10.1074/jbc.M110.200311) [Medline](#)
30. N. L. Price *et al.*, SIRT1 is required for AMPK activation and the beneficial effects of resveratrol on mitochondrial function. *Cell Metab.* **15**, 675 (2012). [doi:10.1016/j.cmet.2012.04.003](https://doi.org/10.1016/j.cmet.2012.04.003) [Medline](#)
31. B. C. Smith, W. C. Hallows, J. M. Denu, A continuous microplate assay for sirtuins and nicotinamide-producing enzymes. *Anal. Biochem.* **394**, 101 (2009). [doi:10.1016/j.ab.2009.07.019](https://doi.org/10.1016/j.ab.2009.07.019) [Medline](#)